MILITARY TECHNICAL ACADEMY "FERDINAND I"

Aircrafts and Military Vehicles Faculty

Habilitation Thesis
(Summary)

Optimal Design and Performances Evaluation of Aircrafts and Turbojet Engines

Scientific Domain
Aerospace Engineering

Author
Professor **Constantin ROTARU**, PhD
"Henri Coandă" Air Force Academy

Bucharest, 2019

Contents (Summary)

Overview

The present Habilitation Thesis, entitled "**Optimization Design and Performances Evaluation of Aircraft and Turbojet Engines**" is based on my achievements and contributions in the aerospace field and reflects my ability for future developments and approaches in this complex and multidisciplinary field. The thesis promotes the need for advanced, analytical and experimental studies in innovative areas, the development of practical tools and the promotion of excellence in the aerospace field.

My scientific and professional achievements after obtaining my doctoral degree in engineering, in the field of aerospace, represent a consequence of the accumulation of knowledge in the technical (engineering) and analytical (mathematics) fields that have enabled me with advanced research skills of some complex physical phenomena. The key terms that could describe my scientific activity might be summed up in: **applicability, complexity, dynamism and multidimensionality**. The arguments that support my scientific activity are represented by real data (articles, books, research contracts, citations, visibility and international recognition) as well as relevant information regarding my involvement in the management of educational and scientific research activities (I have held management positions at the Military Technical Academy: 2005-2014, Head of the Department of Aviation and Mechanics), at "Henri Coandă" Air Force Academy: 2017-2018, Head of the Aviation Department, and since 2018 - until now, I have been the Dean of the Faculty of Aeronautical Management, at "Henri Coandă" Air Force Academy.

The Habilitation Thesis presents the main scientific, professional and academic achievements, after defending the Doctoral Thesis in 1996, at the Military Technical Academy, the Faculty of Aviation and Armored Vehicles, as well as the future research directions I am considering. The main field of research of the author is in the aerospace field, a complex and multidisciplinary field including applications in physics, mathematics, thermodynamics, and fluid mechanics. The chief professional achievements were completed in the fields of the flight dynamics of airplanes and helicopters and in the area of propulsion systems, with a focus on combustion. The thesis summarizes the results obtained in the aerospace field, placing them in the perspective of the priorities of aviation development in order to highlight the preparation and adaptation to the new trends in scientific research.

The thesis is structured into three chapters to which the corresponding bibliographic references are added, the scientific achievements being presented as advanced research studies, some of them having already been published in specialized journals. The content of the Habilitation Thesis provides an overview of my professional training, scientific skills as well as my vision of the evolution of aviation technology and aerospace perspectives. It also illustrates the complexity of the topics addressed, the international dimension and the high degree of novelty.

My professional development included a wide range of didactic and scientific research activities as well as my involvement in administrative activities, management of educational and scientific research activities, organization of scientific events, review of scientific publications, project evaluation and educational and research infrastructure development. All of these are presented in the context of the current approaches in the aerospace field, of the research directions in the field of airplanes, helicopters as well as in the air-jet propulsion systems.

The scientific research carried out after obtaining the title of doctor was based on the creation of mathematical models applicable to the flight dynamics of airplanes and helicopters and to the thermo-gas-dynamics of the propulsion systems, able to lead to the identification of parameters by means of which the calculation of flight performances can be optimized as well as the design process. Solutions were searched for leading to advanced mathematical models, situated, in terms of the level of complexity, above the classical ones presented in the specialized literature. An extended area of research has been that of combustion chambers for turbojet engines.

In the chapter regarding the mathematical models used in the aerodynamics of the airplane, the physical phenomena specific to the air flow around the control surfaces of the plane are treated, the lifting line being associated to the coefficients of a Fourier series. Moreover, the conclusions of a study regarding the dynamic characteristics of the flow around an aerodynamic profile are presented, where the boundary conditions are time dependent. A major factor in the rapid development of airplanes was the evolution of the calculus technology and implicitly of the specialized software programs. The studies we have carried out are based on advanced computing programs that allow a large volume of computation, solving differential equations and operating capabilities with large volumes of databases. There are also presented variants of increase of the coefficient of lift for different aerodynamic configurations, being analyzed the aerodynamic profile with cavity in the upper part, in order to delay the phenomenon of separation of the air fillets from the profile. Regarding the aerodynamics of the propeller, the mathematical models for calculating the velocity induced by the propellers in the composite, forward and rotational movements were analyzed.

The aerodynamics of the helicopter's main rotor is another important area of study, given that the helicopter's flight speed is limited by two factors: the former, related to exceeding the Mach number on the rotor half-disc where the blade is advancing, and the latter related to exceeding the angle of attack on the rotor half-disc where the blade retreats. A special subchapter is dedicated to the coaxial rotor, for the study of which a mathematical model of calculation of the necessary powers was constructed, in order to compare it with the main rotor of a single rotor and tail rotor helicopter.

The sub-chapter "Mathematical models applied to the aircraft gas turbine engines" presents the mathematical model of the aircraft-engine-pilot assembly, this model including a transfer function built on the basis of experimental data in which the pilot’s reaction time and the responses of an aircraft are estimated for the roll, pitch and yaw. The operating limits of the engine are analyzed on the basis of the diagram called the compressor characteristic in which the limits on the surge line, as well as the limits for acceleration and deceleration are presented. The differential equations for the engine movement were written considering the general case of the two spools engine, and a simplified mathematical model was constructed that would allow a quick analysis of the reaction time of the engine to the throttle control. The case studies include response of the engine to step and impulse signals.

The combustion chamber of the engine was analyzed starting from a standard model for the turbojet engine, being built some geometry of the combustion chamber similar to a real engine with 24 injectors. The holes on the circumference of the flame tube were made so that a uniform temperature field was obtained, with higher values toward the outside zone of the combustion chamber, which may lead to lower thermal stresses at the base of the turbine blade. The calculation methodology is based on an extended combustion model, in which a combustion chamber is included featuring the turbine engine, aiming to accelerate the combustion gases, and thus, the denominator of the pressure ratio from the turbine can be reduced.

Regarding the didactic activity carried out after obtaining the scientific title of doctor in the field of aerospace engineering, this was divided into two distinct levels, namely: specialized courses in the aerospace field (Airplane and helicopter aerodynamics, Flight mechanics, Aviation engine theory, Automation of aircraft engine) and respectively, courses in the fundamental field of engineering technical training: Fluid mechanics, Numerical methods of calculation, Computer-based designing, etc.

Starting with my promotion by competition to the didactic position of a university lecturer, the range of disciplines that I taught gradually narrowed to two major areas of interest represented by the *Aerodynamics and flight dynamics* and respectively, the *Construction and operation of airplanes and helicopters*, the aircraft being analyzed as “ a system " including the basic installations: the system of propulsion, hydraulics, fuel, pneumatic, navigation and communications, armament, as well as the control and flight simulation part. Within the Master’s program "Aeronautical Systems Engineering" I have carried out didactic activities for the discipline *Computational Aerothermodynamics*.

From the perspective of the didactic material designed to support the training of Bachelor’s and Master’s students, etc., within the three basic disciplines (*Aerodynamics, Flight mechanics, Aircraft construction and operation)* mentioned above, since 1991 and up to now, I have authored 11 books / specialized manuals published by prestigious national technical publishing houses. In addition, in line with the practical training of students in the same disciplines, I am the author of 3 laboratory platforms (the aircraft fuel installation, the landing gear installation and the hydraulic airplane installation) and of 12 calculation applications based on the ANSYS and MAPLE software programs.

As a scientific coordinator, I have coordinated 40 Romanian and 16 foreign students (ENSIETA-Brest and Saint-Cyr, France and "Paul Sabatier" -Toulouse, France). Also, I have supervised the dissertation theses of masteral students and respectively, engineer-trainee officers within specialized training courses. Furthermore, I have been an official referent in 40 commissions for the public defense of doctoral theses at other universities in the country and in 20 competition commissions for the higher-education positions of professor and associate professor.

Without fear of error, I personally consider that a prolific scientific research activity, with consistent and certified results, is in fact the engine, the essence in the professional evolution of a university professor. Thus, the scientific research activity involves, on the one hand, a thorough and continuous documentation in the specialized literature in the field, and on the other hand, an important intellectual effort for generating professional and scientific contributions in the area of interest. And last but not least, the scientific research activity through its actual results, contributes to the increase of the individual professional visibility, yet, to a significant extent, it also contributes to the prestige of the institution where I belong.

I carried out scientific research tasks as a director / project manager or as a project member in the research groups established at the Military Technical Academy and in collaboration with the aviation institutes COMOTI, INCAS, the Polytechnic University of Bucharest and the Romanian Space Agency.

Complementarity and interdisciplinarity of the research

As it can be noticed from the list of scientific papers, all the topics addressed that have been the object of my scientific research are related to a greater or lesser extent to the "aircraft-engine" system, in which parameters that directly influence the aircraft and the propulsion system are highlighted and more than that, there are identified parameters on which the flight qualities of the aircraft (aircraft or helicopters) depend. The mathematical models used allowed the extension of the area of analysis of the flight performances, the basic factors on which they depend and which can influence the operational capabilities of the aircraft being discovered.

2. SCIENTIFIC AND RESEARCH ACTIVITY RESULTS

2.1 Mathematical models used in the airplane aerodynamics

2.1.1 Mathematical model of induced flow on the airplane vertical tail

This mathematical model is built starting from the separate formulation of the Fourier coefficients in the series solution of the Prandtl's lifting-line equation and the numerical results are obtained in Maple soft environment, for a standard configuration of an airplane geometry for induced flow on the airplane vertical tail, including of the vortex model for the sidewash gradient on the vertical stabilizer.

An aircraft moving through the air will experience drag that opposes the motion and if the angle of attack remains constant, this drag increases with increasing air velocity, while the thrust developed by an aircraft engine is either constant with airspeed or decreases with increasing airspeed, so, the forward component of thrust must balance the drag when an airplane is in static equilibrium with regard to translation in the direction of motion. The airplane is unstable for disturbances in normal velocity and any disturbance of velocity in a direction normal to the equilibrium flight path will result in an aerodynamic force that opposes the disturbance. It is easier to design an unmanned aircraft with an autopilot than it is to design a good manned airplane, from an analytical point of view.

The primary importance for maintaining airplane trim is the static stability in the rotational degrees of freedom and any disturbance in roll, pitch or yaw must all result in the production of a restoring moment that will return the airplane to the original equilibrium attitude in order to be statically stable in rotation. The net side force, rolling moment and yawing moment must all be zero for equilibrium longitudinal motion, the airplane having a positive sideslip when the component of airplane velocity relative to the surrounding air is positive. In reality no airplane can be always be perfectly symmetric, asymmetric loading and thrust, propeller rotation or an asymmetric distribution of bugs on the wings can cause either inertial asymmetry or aerodynamic asymmetry, thus, ever for level flight, some provision must be made for trimming the airplane in roll and yaw. A yaw disturbance in a positive sideslip angle requires a positive yawing moment to restore the disturbance to zero for a standard configuration of an airplane geometry, so, static stability in yaw requires that $C_{n,\beta} = \partial C_n / \partial \beta > 0$, in mathematical terms. Good performances and handling qualities are normally found with $C_{n,\beta}$ in the interval between 0.06 and 0.15 per radian, for a typical airplane configuration, the size of the vertical tail being not usually fixed by consideration of static stability, and sufficient static stability is normally provided when the vertical tail is sized based on control and dynamic handling quality requirements.

The sidewash gradient is negative and has a stabilizing effect on the airplane for a vertical tail mounted above the wing, and it has a significant effect on the static yaw stability of an airplane. The y component of velocity induced by the pair of wingtip vortices at an arbitrary point in space (x, y, z) can be estimated using the vortex model (fig. 1) and Biot-Savart law, as it follows

$$V_y = \frac{\Gamma_{wt}}{4\pi}\frac{z}{z^2+\left(y+\frac{1}{2}b'\right)^2}\left(1+\frac{x-\frac{1}{2}b'\tan\Lambda}{\sqrt{A}}\right)-\frac{\Gamma_{wt}}{4\pi}\frac{z}{z^2+\left(y-\frac{1}{2}b'\right)^2}\left(1+\frac{x-\frac{1}{2}b'\tan\Lambda}{\sqrt{B}}\right) \tag{1}$$

where

$$\begin{aligned} A &= \left(x-\frac{1}{2}b'\tan\Lambda\right)^2+z^2+\left(y+\frac{1}{2}b'\right)^2 \\ B &= \left(x-\frac{1}{2}b'\tan\Lambda\right)^2+z^2+\left(y-\frac{1}{2}b'\right)^2 \end{aligned} \tag{2}$$

The spacing b' and vortex strength Γ_{wt} can be calculated from Prandtl's lifting line theory, taking into account that the wingtip vortex strength is proportional to the product of the wing lift coefficient and airspeed.

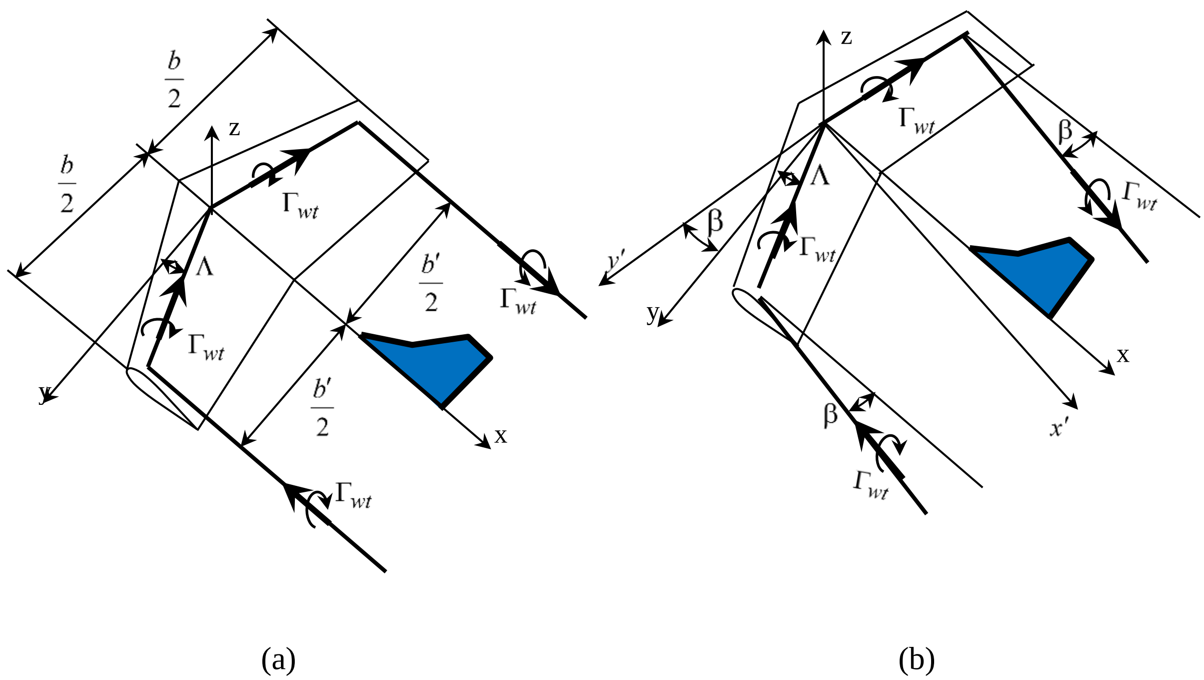

Fig. 1. Model of the wing tip vortex (a) and his effect of the sideslip (b)

According to the sign convention used in the vector calculus (the sidewash is positive from left to right) and applying the small angle approximation, the sidewash angle can be written as

$$\varepsilon_s = -\frac{V_y}{V_\infty} = \frac{C_{Lw}k_v}{\pi^2\lambda_w}\frac{\bar{z}}{\bar{z}^2+\left(\bar{y}-k_b\right)^2}\left(1+\frac{\bar{x}-k_b\tan\Lambda}{\sqrt{\bar{A}}}\right)-\frac{C_{Lw}k_v}{\pi^2\lambda_w}\frac{\bar{z}}{\bar{z}^2+\left(y+k_b\right)^2}\left(1+\frac{\bar{x}-k_b\tan\Lambda}{\sqrt{\bar{B}}}\right)$$

where C_{Lw} and λ_w are the lift coefficient and aspect ratio for the wing and

$$\begin{aligned}
\bar{x} &= \frac{x}{b_w/2},\ \bar{y} = \frac{y}{b_w/2},\ \bar{z} = \frac{z}{b_w/2}; \\
\bar{A} &= (\bar{x} - k_b \tan\Lambda)^2 + \bar{z}^2 + (\bar{y} - k_b)^2; \\
\bar{B} &= (\bar{x} - k_b \tan\Lambda)^2 + \bar{z}^2 + (\bar{y} + k_b)^2
\end{aligned} \tag{3}$$

On the other hand, the parameters k_v and k_b can be represented in the form

$$k_v = 1 + \sum_{n=2}^{\infty} \frac{A_n}{A_1} \sin\left(n\frac{\pi}{2}\right);\quad k_b = \frac{\dfrac{\pi}{4} + \sum\limits_{n=2}^{\infty} \dfrac{nA_n}{(n^2-1)A_1} \cos\left(n\dfrac{\pi}{2}\right)}{1 + \sum\limits_{n=2}^{\infty} \dfrac{A_n}{A_1} \sin\left(n\dfrac{\pi}{2}\right)} \tag{4}$$

where A_1, A_2,......A_n are the Fourier coefficients in the series solution to Prandtl's lifting-line equation. A major factor in the rapid development of aircraft technology consisted in the ability to develop computers methods in performance calculation but the results may often not be greatly different from those derived from the simple analytical formulae and the fact that the feasibility of calculation is not dependent upon making a large number of challengeable assumptions is important in pinning down a design, making comparisons with flight tests. In the fig. 2 is represented an unsteady motion of the surface on which the "zero normal flow" boundary condition is applied, the motion of the origin being prescribed in an inertial frame of reference (*X*, *Y*, *Z*). The relative motion of the origin of the body fixed frame of reference is prescribed by its location (X_0, Y_0, Z_0) at $t > 0$ with the instantaneous orientation $\Theta(t) = (\varphi, \theta, \psi)$, where (φ, θ, ψ) are the Euler rotation angles. The fluid surrounding the body is assumed to be incompressible, inviscid and irrotational over entire flow field, excluding the body's solid boundaries and its wake.

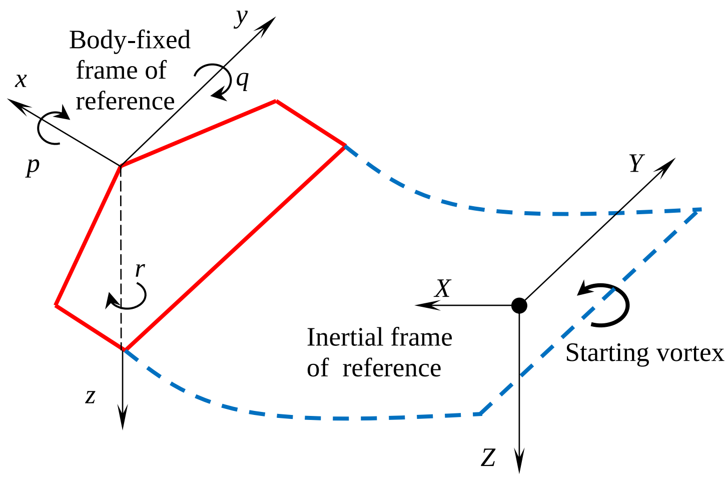

Fig. 2. Coordinate systems

In the inertial frame of reference, the continuity equation becomes $\nabla^2\Phi = 0$ and the boundary condition requiring zero normal velocity across the body's solid boundaries is

$$(\nabla\Phi + \vec{v})\cdot n = 0 \qquad (5)$$

where $\vec{n}(x, y, z, t)$ is the unity vector normal to this moving surface and $\vec{v}$ is the surface velocity (v is defined with minus sign so that the undisturbed flow velocity will be positive in the body's frame of reference). The time dependency of equation $\nabla^2\Phi = 0$ is introduced through the boundary condition because the location and orientation of $\vec{n}$ can vary with time and a second boundary condition requires that the flow disturbance due to the body's motion through the fluid, should diminish far from the body, $\lim_{|R-R_0|\to\infty} \nabla\Phi = 0$, where $R = (X, Y, Z)$. The Kelvin equation can be used to determine the stream wise strength of the vorticity shed into a wake, so, it could be an additional condition for the unsteady flow, based on the remark that the circulation Γ around a fluid curve enclosing the body and its wake is conserved, $d\Gamma / dt = 0$. A transformation from (X, Y, Z) coordinate system to (x, y, z) coordinate system should include the translation and the rotation of the (x, y, z) system and may have the following form

$$\begin{pmatrix} x \\ y \\ z \end{pmatrix} = \begin{pmatrix} 1 & 0 & 0 \\ 0 & \cos(\varphi(t)) & \sin(\varphi(t)) \\ 0 & -\sin(\varphi(t)) & \cos(\varphi(t)) \end{pmatrix} \times \begin{pmatrix} \cos(\varphi(t)) & 0 & -\sin(\varphi(t)) \\ 0 & 1 & 0 \\ \sin(\varphi(t)) & 0 & \cos(\varphi(t)) \end{pmatrix} \times \begin{pmatrix} \cos(\varphi(t)) & \sin(\varphi(t)) & 0 \\ -\sin(\varphi(t)) & \cos(\varphi(t)) & 0 \\ 0 & 0 & 1 \end{pmatrix} \times \begin{pmatrix} X - X_0 \\ Y - Y_0 \\ Z - Z_0 \end{pmatrix} \qquad (6)$$

A numerical approach to correct for this wake discretization error is to place the latest vortex closer to the trailing edge, namely the placement of the discrete vortex at the middle of the interval $U(t)\Delta t$. According to the Helmholtz theorem, there is no vortex decay, that is, if a wake vortex element is shed from the trailing edge, its strength is conserved. the combined airfoil and wake induced velocity $(u, w)_i$. The combined airfoil and wake induced velocity $(u, w)_i$, at each time step, is calculated and the vortex elements are moved by $(\Delta x, \Delta y) = (u, w)_i \Delta t$, the coordinate system (x, z) beings selected such that the x coordinate axis is tangent to the path and the origin is placed on the path. In the assumption that the path radius of curvature is much larger than the chord c, the airfoil camber line is given in this coordinate system by $\eta(x, t)$, which is considered to be small $(\eta / c << 1)$. The relative angle to the trailing edge and the distance are important numerical parameters, the wake vortex location should be closer to the position of the trailing edge. No normal flow across the surface is given by the expression $(\nabla\Phi - \vec{V}_0 - \vec{v}_{rel} - \vec{\Omega}\times\vec{r})\cdot\vec{n} = 0$, where $\Phi = \Phi_B + \Phi_w$ is the equivalent of the steady-state velocity potential, divided into airfoil potential Φ_B and to a wake potential Φ_w. The parameter $\vec{V}_0$ is the instantaneous velocity of the coordinate system origin, $V_0 = [-U(t), 0, 0]$, $\vec{\Omega}$ is the instantaneous rotation, $\Omega = [0, \dot{\theta}(t), 0]$, $\vec{v}_{rel}$ is the relative velocity of the chord line within coordinate system (x, y, z), $v_{rel} = \left[0, 0, \frac{\partial \eta}{\partial t}\right]$, and $\vec{n}$ is the normal vector to the surface

$$n = \left[-\frac{\partial \eta}{\partial x}, 0, 1\right] / \sqrt{\left(\frac{\partial \eta}{\partial x}\right)^2 + 1} \tag{7}$$

The wake potential being known from the previous time steps, then

$$\frac{\partial \Phi_B}{\partial z} = \left(\frac{\partial \Phi_B}{\partial x} + \frac{\partial \Phi_w}{\partial x} + U - \dot{\theta} z\right)\frac{\partial \eta}{\partial x} - \frac{\partial \Phi_w}{\partial z} - \dot{\theta} x + \frac{\partial \eta}{\partial t} \tag{8}$$

With assumptions presented above, the downwash induced by the airfoil bound circulation $\gamma(x, t)$ is

$$\frac{\partial \Phi_B}{\partial z} = -\frac{1}{2\pi}\int_0^c \frac{\varphi(x_0, t)}{x - x_0} dx_0 \tag{9}$$

The time dependent equivalent of the steady-state boundary condition is represented by the equation

$$-\frac{1}{2\pi}\int_0^c \frac{\varphi(x_0, t)}{x - x_0} dx_0 = U(t)\frac{\partial \eta(x, t)}{\partial x} - \frac{\partial \Phi_w}{\partial z} - \dot{\theta}(t) \cdot x \frac{\partial \eta(x, t)}{\partial t} \tag{10}$$

with the Kutta condition $\gamma(c, t) = 0$.

A similar solution to the vortex distribution can be obtained, with the classical approach of Glauert, namely,

$$\gamma(\theta, t) = 2U(t)\left[A_0(t)\frac{1 + \cos\theta}{\sin\theta} + \sum_{n=1}^{\infty} A_n(t)\sin n\theta\right] \tag{11}$$

where

$$A_0(t) = -\frac{1}{\pi}\int_0^{\pi} \frac{w(x, t)}{U(t)} d\theta \text{ and } A_n(t) = \frac{2}{\pi}\int_0^{\pi} \frac{w(x, t)}{U(t)} \cos n\theta d\theta \tag{12}$$

The aerodynamic lift force per unit span L' and the pitching moment about the airfoil's leading edge M_0 have the expressions

$$L'(t) = \pi\rho c\left\{\left[U^2 A_0 + \frac{3c}{4}\frac{\partial}{\partial t}(U A_0)\right] + \left[U^2 \frac{A_1}{2} + \frac{c}{4}\frac{\partial}{\partial t}(U A_1) + \frac{c}{8}\frac{\partial}{\partial t}(U A_2)\right]\right\} \tag{13}$$

$$\begin{aligned} M_0(t) = &-\rho c^2 \frac{\pi}{2}\left[\frac{U^2}{2} A_0 + \frac{7c}{8}\frac{\partial}{\partial t}(U A_0) + \frac{U^2}{2} A_1 + \frac{3c}{8}\frac{\partial}{\partial t}(U A_1)\right] - \\ &-\rho c^2 \frac{\pi}{2}\left[-\frac{U^2}{4} A_2 + \frac{c}{8}\frac{\partial}{\partial t}(U A_2) - \frac{c}{32}\frac{\partial}{\partial t}(U A_3)\right] \end{aligned} \tag{14}$$

2.1.2 Lift capability prediction for aerodynamic configuration

This chapter presents a mathematical model of the flow around the helicopter rotor airfoil in order to predict the lift capability, where the proposed solution consists in an airfoil with filled cavity, where the filled body is a rotating cylinder, being generated a series of vortices that reduce the flow separation downstream of the cavity. The possibility of a delay in flow separation on the upper surface for the retreating blade was appeared as a result of the comparation between the CFD results with those obtained by panel method. This new airfoil type could improve the lifting capability of the rotor blade and may lead to new rotors optimized for greater performances in both hover and high speed forward flight taking into account that the advancing blade operates at low angle of attack but at high subsonic or transonic conditions, whereas the retreating blade operates at low Mach numbers and high lift coefficients.

At high angle of incidence and compressibility effects at high Mach number, the envelope of rotor thrust limits is the outcome of operation on the blades of stall effects. Because of the drop in dynamic pressure which limits the thrust achievable throughout the forward speed range, maximum thrust on the retreating blade falls and by the converse effect, maximum thrust possible on the advancing side increases but is unrealizable because of the retreating blade restriction. As the advancing tip Mach number approaches 1.0, its lift becomes restricted by shock-induced flow separation, leading to drag or pitching moment divergence, which limits the maximum speed achievable, therefore, the envelope comprises a limit on thrust from retreating blade stall and a limit on forward speed from advancing blade Mach effects.

Airfoil blade with filled cavity

A standard NACA 2412 airfoil with and without cavity was used for two-dimensional simulations. In order to fix the separation point (forward edge) and to maximize the feedback loop of the shear layer (rear edge), both edges of the cavity were sharp. For improving the circulation around the airfoil, the cavity was filled with a rotating small cylinder (fig. 3).

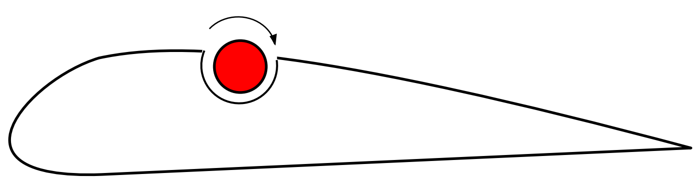

Fig. 3 Filled airfoil cavity

In order to assess convergence and influence of the far-field boundary condition, the grid resolution and domain size were varied, the computational domain was extended to a distance of 12 chords lengths in the upstream and downstream directions and three chords lengths in the upper and lower normal directions and also, the Reynolds number was sufficiently high such that the formation of large scale vortices and the subsequent pairing of these structures gave rise to aperiodic low frequency oscillations (that are difficult to characterize because the run times are not sufficiently long to observe many periods).

In fig. 4 is presented the pressure distribution on the airfoil.

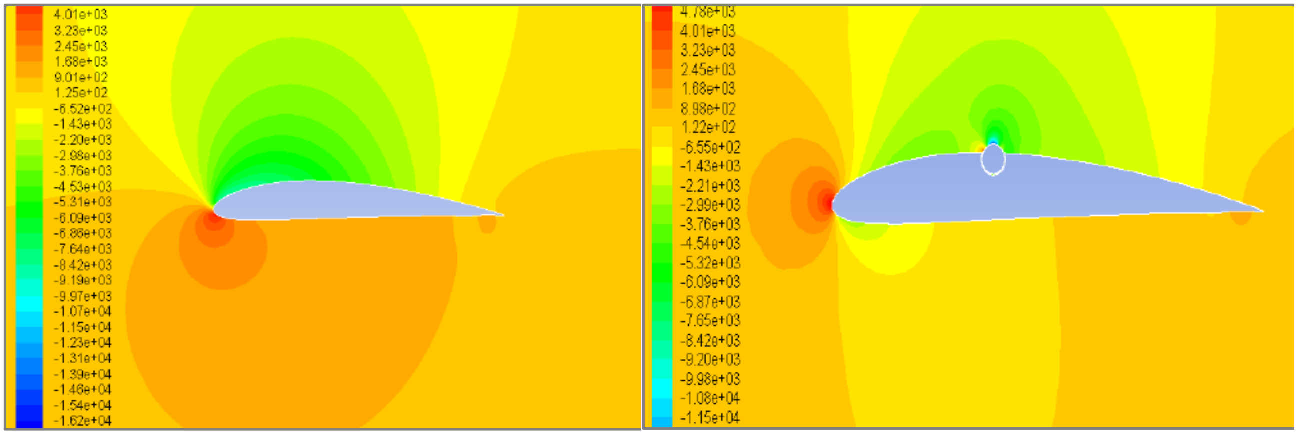

Pressure distribution on the airfoil without cavity   Pressure distribution on the airfoil with cavity

Fig. 4

Approximately at the half chord length from the leading edge, the relative high thickness of the airfoil without cavity causes a laminar separation and at very high angles of attack the flow over the airfoil with cavity separates well before the forward edge of the cavity. There is a strong interaction in the cavity between the streamlines and this interaction causes the flow to shed smaller scale structures than the airfoil without cavity at the same angle of attack.

The separated vortices tend to merge into larger structures before being shed into the wake, for the clean airfoil at $\alpha = 0^\circ$ the flow initially separates around 50% of the chord length and this separation causes a periodic vortex shedding in the wake of the airfoil. On the other hand, at $\alpha = 10^\circ$ and $\alpha = 15^\circ$ the vortex structures and the separation bubble are larger and the separation point on the suction side moves upstream with increasing the angle of attack. For low Mach numbers and small angles of attack the section lift coefficients predicted by thin airfoil theory and panel codes are in good agreement with experimental data.

2.1.3 New solutions for aircraft wing and helicopter blade airfoils

An airfoil design problem begins with a set of aerodynamic requirements that include lift, drag and pitching moment in a specified Mach/Reynolds number flow regime plus geometric constraints on thickness, and the applicability of section data to the prediction of the aerodynamic characteristics of wings is limited by the simplifying assumptions made in the development of wing theory. In the development of the lifting-line theory, it was assumed the effect of the trailing vortices was to change the local angle of attack, neglecting any change of downwash along the chord of the section, therefore, the sections are operating in a curved as well as rotated flow field whenever the spanwise variation of lift is not small.

The rotor limits may be determined by either retreating blade stall or advancing blade compressibility effects, two operation conditions being valid, one condition given by advancing blade compressibility effects and the other one condition given by retreating blade stall, in either case the retreating blade operates at low Mach numbers and high lift coefficients and the advancing blade operates at low angle of attack but at high subsonic or transonic conditions. There has been a great deal of emphasis in rotor design on maximizing the lifting capability of rotor airfoil sections to simultaneously alleviate both compressibility effects and retreating blade stall, because the onset of flow separation may limit rotor performance

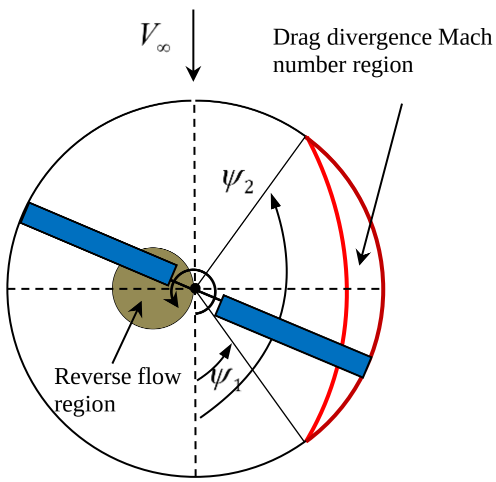

Fig. 5 Helicopter rotor blade

Figure 5 shows the region of the rotor disk affected by compressibility effects being defined on the surface where the incident Mach number of the flow that is normal to the leading edge of the blade exceeds the drag divergence Mach number, M_{dd} . The region of the disk affected by compressibility effects is defined by the expression

$$M_{r,\psi} = M_{\Omega R}\left(r + \mu \sin\psi\right) \geq M_{dd} \tag{15}$$

According to fig. 5, one aerodynamic effect with helicopter rotors is that the tip vortices from one blade can lies close to other and to the plane of blade rotation so, they have large induced effects on the blade lift distribution. A rotating cylinder was modeled for the cavity in order to improve the circulation around the airfoil. In figs. 6, 7, 8 and 9 are shown some interesting results regarding the pressures and velocities.

Airfoil model

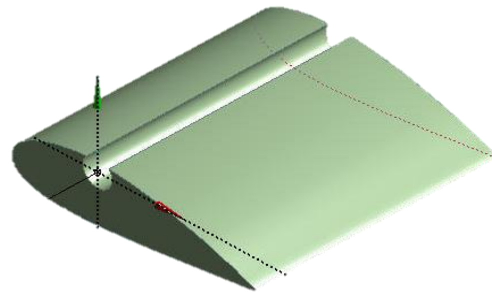

Cavity profile

Fig. 6

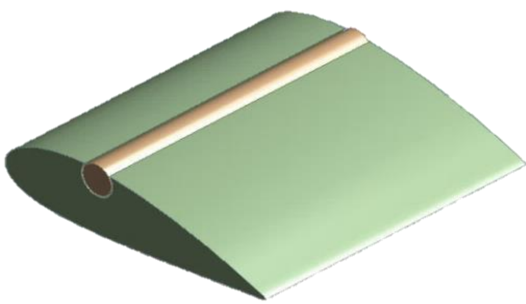

Filed cavity

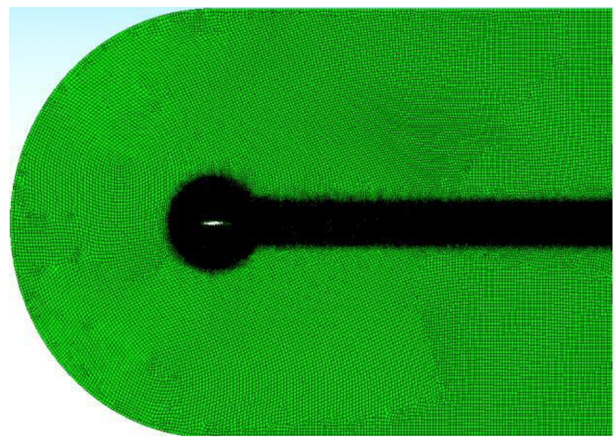

Mesh domain

Fig. 7

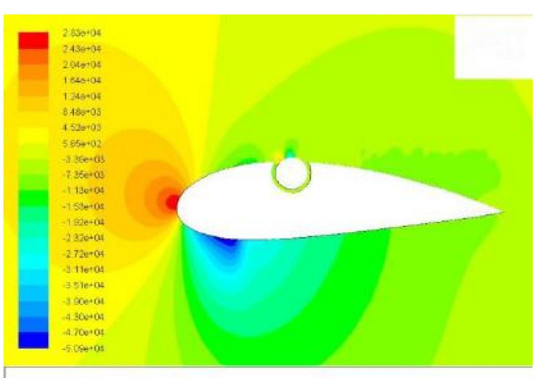

Static pressure

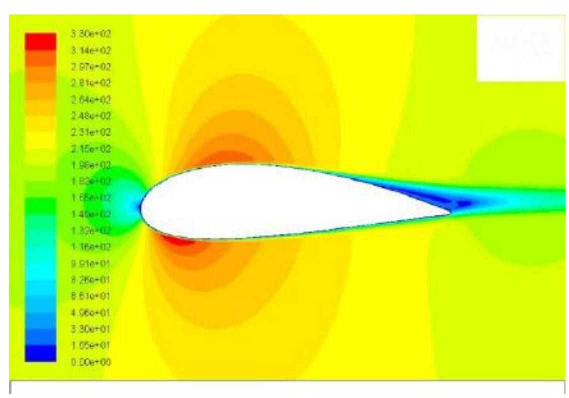

Velocity magnitude

Fig. 8

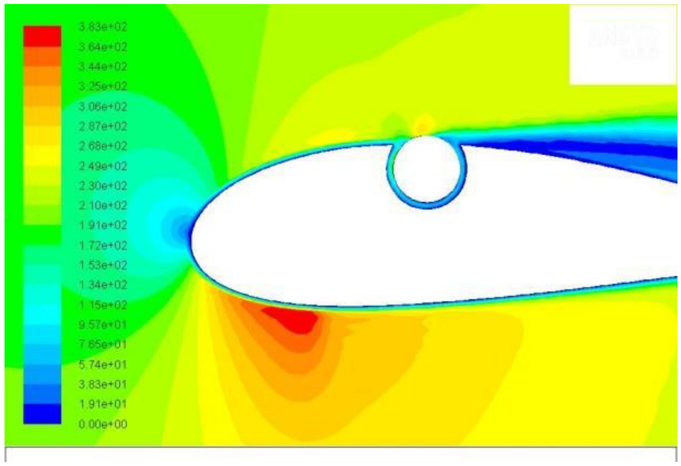

Fig. 9 Static pressure

A laminar separation which initially starts approximately half a chord length from the leading edge is caused by the relative high thickness of the airfoil without cavity and at high angles of attack the flow over the airfoil with cavity separates before the forward edge of the cavity. This solution could be applied in order to avoid flow separation and to get improved performances, especially at low velocities, like in the take-off or landing operation.

2.1.4 Airplane propeller aerodynamic design and performances analysis

The airplane performances, stability and its control are directly related on development and improvement of propulsion systems technology, the developed thrust being regarded as a reaction force resulted from the momentum and kinetic energy increase of the air which passes through the engine. The equation of the thrust T, is obtained by applying Reynolds Transport Theorem to a control volume that extends sufficiently far from the propulsion system, so that at the boundary enclosing this volume the air pressure is equal to the ambient (atmospheric) pressure. From the above equation it results that the thrust developed by any propulsion system can be increased either by acting upon the velocity increment or upon the mass flow rate but the most increasing thrust is obtained by using a large mass flow rate with a small velocity increment (fig. 10), this type of propulsion system being the most efficient device commonly used for low speed subsonic flight. Besides others improvements of blade aerodynamic shapes or of movement transmission mechanisms which connect the propeller and the reciprocating or turboshaft engines, one important development in aviation was the introduction of the variable-pitch propellers.

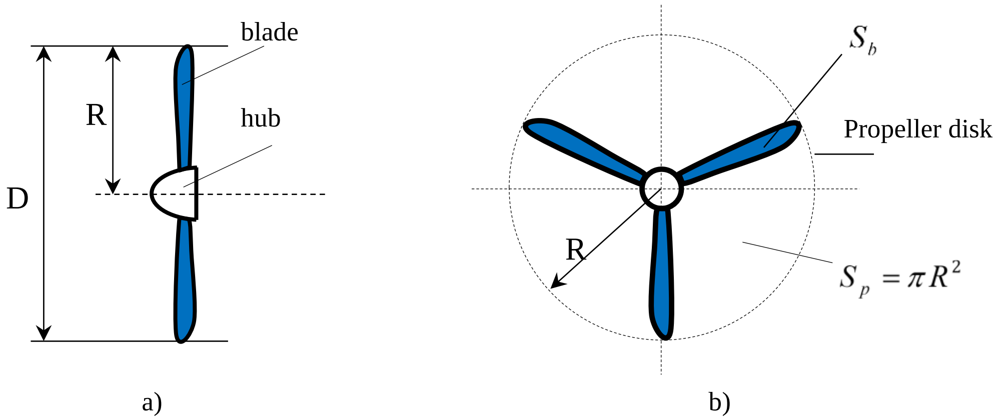

Fig. 10 Propeller geometry: a) lateral view, b) front view

The lift developed by a propeller is oriented with the direction of motion whereas the lift force developed by a wing is directed to support the airplane weight and keep it aloft, the relative airflow over a propeller blade being a result of its rotation movement, so that, the velocity of each section depends on the distance from the axis of rotation, the propeller blade having much more twist or geometric washout than a conventional wing.

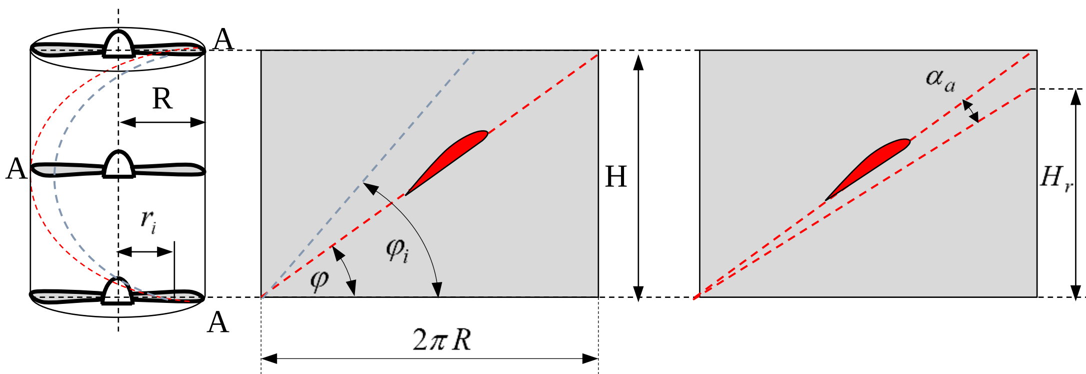

Fig. 11 Theoretical pitch (H) and actual pitch (H_r)

The axial component of the airplane airspeed affects the aerodynamic forces and moments acting on the rotating propeller because this component of the airspeed is normal to the plane of rotation and it changes the blades angle of attack, in a rotation movement each blade acts behind the blade that precedes it.

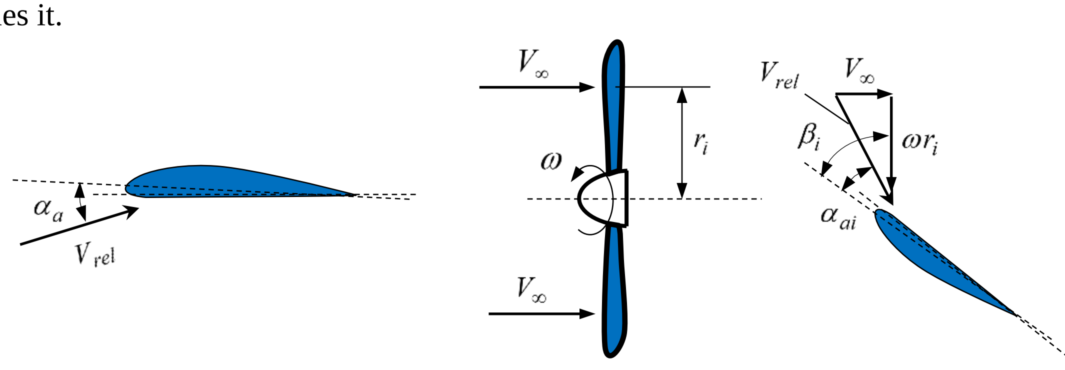

Fig. 12 Velocities triangle

The pressure difference acting on the air, generates a momentum in a direction opposite to the aerodynamic force acting on the propeller, so, the engine-propeller combination regarded as a whole, depends on operating conditions and matching the propeller with the engine as well as the matching with the airframe.

2.2 AERODYNAMIC DESIGN AND PERFORMANCES ANALYSIS FOR HELICOPTERS

Other research direction consists in the study of helicopter rotor blade physical features and the techniques for modeling the unsteady effects found on airfoil operating under nominally attached flow conditions away from stall, the unsteady problem being approached on the basis of Theodorsen theory, where the aerodynamic response (lift and pitching moment) is considered as a sum of a noncirculatory (apparent mass accounts for the pressure forces required to accelerate the fluid in the vicinity of the airfoil) and circulatory parts.

2.2.1 Helicopter rotor blade aerodynamics

In order to predict the aerodynamic behavior of airfoils in the high AoA regime it is important to study the adverse effects produced in the reverse flow regime on the rotor, because in the reverse flow region, the direction of the relative flow vector changes from the trailing edge toward the leading edge of the airfoil and the wakes and tip vortices from on the other blades can lie close to each other and to the plane of blade rotation and so they have large induced effects on the blade lift distribution. In comparation with the fixed wing, the helicopter tip vortices are curved lines, they experience a self-induced effect (fig. 13).

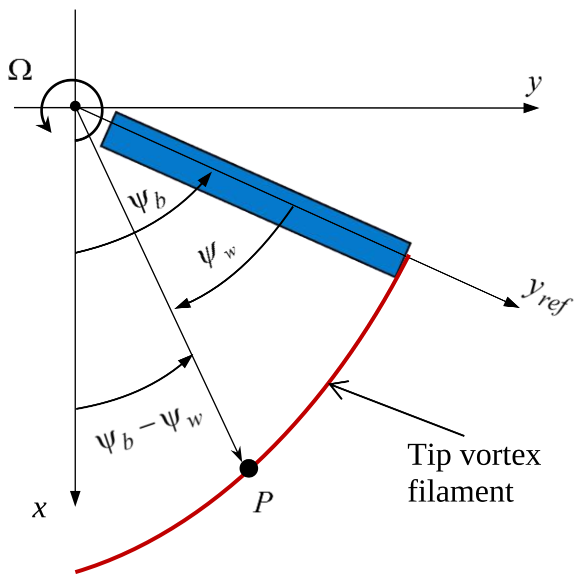

Fig. 13 Tip vortex trajectory

These blade-vortex-interactions can occur at many different locations over the rotor disk and also with different orientations and for they study is used the reduced frequency, *k*, defined as

$k = \omega \cdot c/(2V)$, where c is the chord of the airfoil, ω is the angular frequency and V is the flow velocity. The resultant force, F, generated by an airfoil chord with the chord c, can be written in functional form as $F/(\rho V^2 c^2) = f(\mathrm{Re}, M, k)$. Flows with characteristic reduced frequencies above of 0.05 are considered unsteady (for $k = 0$ the flow is steady and for $0 \le k \le 0.05$ the flow can be considered quasi-steady). The reduced frequency at any blade element can't be exactly calculated, but a first order approximation for k, can give useful information about the degree of unsteadiness. A good level of analysis of the unsteady aerodynamics can be obtained from 2-D thin airfoil theory, but the Laplace's equation for incompressible flow being eliptic, the unsteady aerodynamic theories cannot be obtained in a corresponding analytical form.

2.2.2 The apparent mass tensor for helicopter rotor blade

The external force F_e applied to the body to translate it through the fluid has to be applied in a direction different from that of the acceleration of the body through the fluid, because the rate of change of the impulse vector, in general, is not in the direction of the acceleration of the body, and the boundary conditions that should be satisfied on given frontier of the fluid depend on the assumptions made with regard to the nature of the fluid, more specifically on the nature of the differential equations that are assumed to govern the motion of the fluid. For a surface represented by a scalar function of position and time, $F(\vec{r}, t) = 0$, the total time rate of change is zero,

$$\frac{D(F)}{Dt} = \frac{\partial(F)}{\partial t} + \vec{V} \cdot grad(F) = 0 \qquad (16)$$

on $F(\vec{r}, t) = 0$ and the fluid force acting on a rigid body of arbitrary shape translating with a velocity $\vec{U}(t)$ is given by

$$\vec{F} = -\iint_S p\vec{n}dS \qquad (17)$$

where p is the pressure on the surface of the body and S denotes the surface of the body.

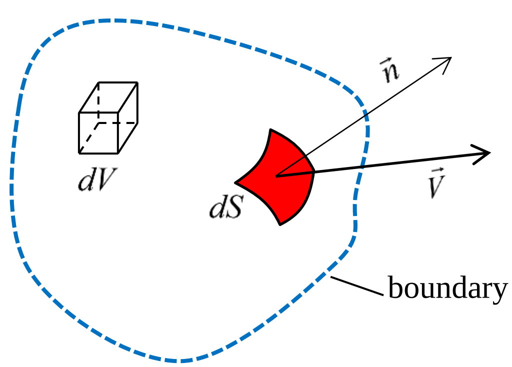

Fig. 14 Solid-fluid surface.

In general, the movement of body may be translating, rotating and deforming, consequently, the velocity U is a function of position on the surface and time, while if the body is rigid and is in translatory motion, then U is a function of time, but uniform over the surface of the body, therefore, the mathematical problem is to determine the externally force $\vec{F}_e$ applied to the body to translate it through the fluid. According to Newton's second law, we have

$$\frac{d}{dt}\left(m\vec{U}\right)=\vec{F}_e+\vec{F} \tag{18}$$

where m is the mass of the body. The equation (18) may be expressed in the form

$$\vec{F}_e=\frac{d}{dt}\left(m\vec{U}\right)-\vec{F} \tag{19}$$

or

$$\vec{F}_e=\frac{d}{dt}\left(m\vec{U}+\vec{I}\right) \tag{20}$$

where $\vec{I}$ is the impulse applied on the fluid and $-d\vec{I}/dt=\vec{F}$.

On the other hand, the fluid force acting on the body is

$$\vec{F}=\frac{\partial}{\partial t}\oiint_S \rho\phi\vec{n}dS-\rho\vec{U}\times\oiint_S \vec{n}\times grad(\phi)dS \tag{21}$$

The impulse applied on the fluid is related on the integral

$$\vec{I}_C=\oiint_S \vec{n}\times grad(\phi)dS \tag{22}$$

where C denotes the circulation around the body and ϕ is the velocity potential.

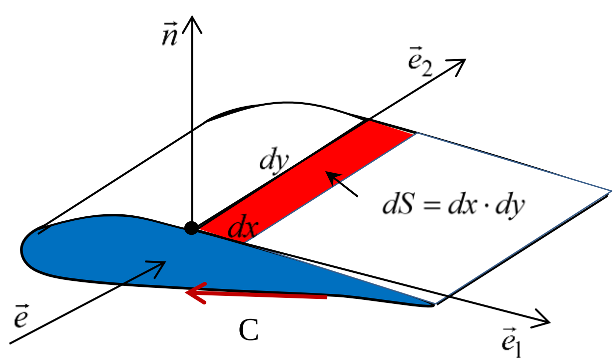

Fig. 15. *Rotor blade element.*

In the figure 15 is represented a blade element with the main unit vectors: the unit vector $\vec{e}$ is normal to the cutting planes, the unit vector $\vec{e}_1$ is tangent to the curve of intersection between the blade element surface and the cutting plane and the unit vector $\vec{e}_2$ is tangent to the blade element surface.

$$\vec{F}_e = \left[(m + m_{11}) \frac{du_1}{dt} + m_{12} \frac{du_2}{dt} + m_{13} \frac{du_3}{dt} \right] \vec{i} + \\ + \left[m_{21} \frac{du_1}{dt} + (m + m_{22}) \frac{du_2}{dt} + m_{23} \frac{du_3}{dt} \right] \vec{j} + \\ + \left[m_{31} \frac{du_1}{dt} + m_{32} \frac{du_2}{dt} + (m + m_{33}) \frac{du_3}{dt} \right] \vec{k} \tag{23}$$

The coefficients m_{ik} form a tensor of nine numbers which may be displayed as an array

$$\begin{pmatrix} m_{11} & m_{12} & m_{13} \\ m_{21} & m_{22} & m_{23} \\ m_{31} & m_{32} & m_{33} \end{pmatrix} \tag{24}$$

being a virtual mass tensor or virtual masses that need to be added to the mass of the body in order to find the force that must be applied to translate it through the fluid. Using the mathematical symbol δ_{ik} defined by $\delta_{ik} = 0$ if $i \neq k$ and $\delta_{ik} = 1$ for $i = k$, equation (23) may be rewritten

$$(F_e)_i = \sum_{k=1}^{3} (m\delta_{ik} + m_{ik}) \frac{du_k}{dt} \tag{25}$$

There are three perpendicular axes such that $m_{ik} = 0$ for $i \neq k$, so with respect to such directions, the equation (25) becomes

$$(F_e)_i = (m + m_{ii}) \frac{du_i}{dt}, \text{ i=1, 2, 3} \tag{26}$$

The expression $(m + m_{ii})$ represents the apparent mass for translation in the i-direction and the corresponding m_{ii} is the additional apparent mass.

Helicopter Configurations

The classical constructive configuration of helicopter is that having one or more engines with gear boxes connected to the engines by rotating shafts to transfer the power from engines to the rotors (fig.16).

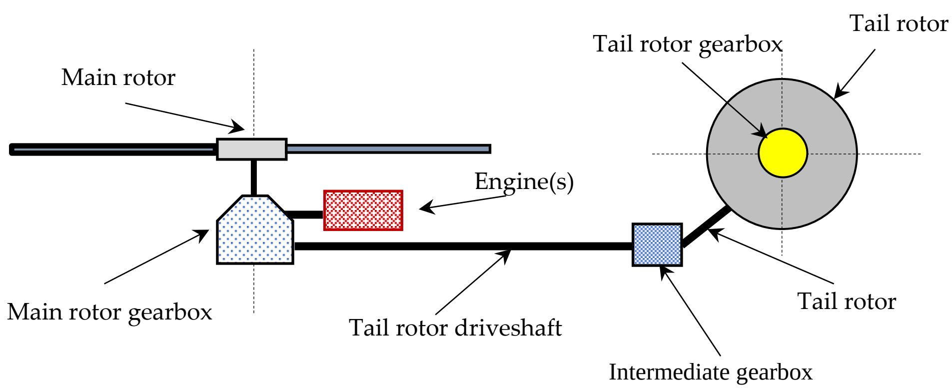

Fig. 16 Typical helicopter constructive model

Basics of Helicopter Aerodynamics

The actuator disc theory is the simplest method that describes the lifting rotor and it assumes the existence of a stream tube which represents an axially symmetric surface passing through the rotor disc perimeter (fig. 17) and also, it is based on achieving a lifting force by generating a change of momentum.

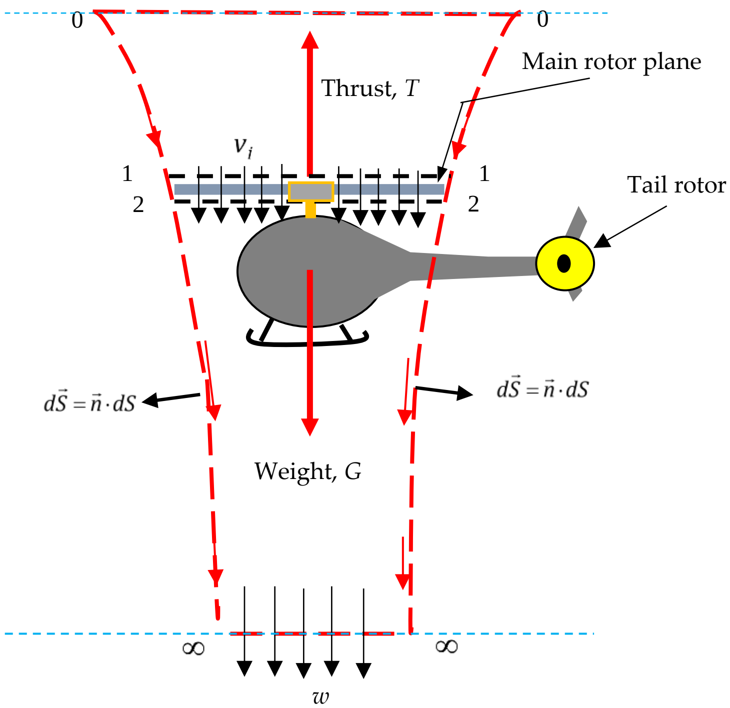

Fig. 17 The main rotor control volume.

The main assumption is that the air is incompressible and the flow remains in the same direction, the helicopter rotor generates a vertical force in opposition to the helicopter's weight and a horizontal propulsive force for forward flight. Also, in order to control the attitude and position, the main and tail rotors generate the forces and moments.

Figure 36 shows the control volume of the main rotor: the plane far upstream of the rotor (section 0-0); the planes just above and below the rotor disc (sections 1-1, and 2-2); the far wake section, denoted by index ∞. The induced velocity through the rotor disk is v_i and in the far wake the air velocity is w, the unit normal area vector is $d\vec{S} = \vec{n} \cdot dS$, with the unit normal area vector $\vec{n}$ is oriented outward the control volume. For any extensive parameter *B*, where $B = b \cdot m$, according to the Reynolds Transport Theorem, the following equation is valid

$$\left(\frac{dB}{dt}\right)_{system} = \frac{\partial}{\partial t} \iiint\limits_{\substack{control \\ volume}} \rho b dV + \iint\limits_{\substack{control \\ surface}} (\rho b) \vec{V} \cdot d\vec{S} \tag{27}$$

where *m* is the mass of fluid $\vec{V}$ is the local velocity and ρ is the fluid density.

Vertical climb

Considering the helicopter in climb, it leaves the hovering condition and moves in a vertical direction, the flow remains symmetrical about the thrust force line, that is normal to the rotor disk, the flow becomes very complex in a medium descent rate condition, but in climb, the mathematical approach is close to that used in the hover conditions.

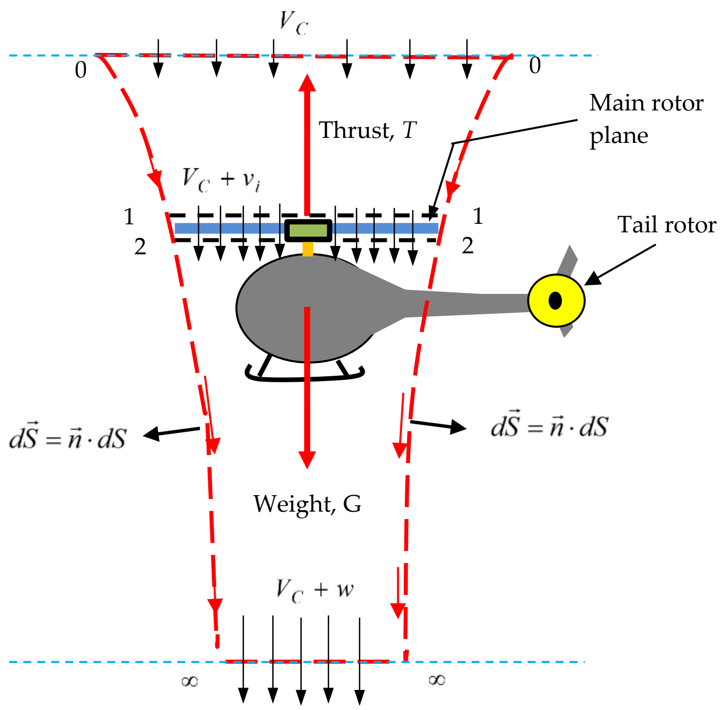

Fig. 18 The axial climbing flight.

Acording to the principles of conservation for mass, momentum and energy it follows that:

$$\dot{m} = \rho A(V_C + v_i); \quad T = \dot{m}w; \quad w = 2v_i \tag{28}$$

Dividing the force T by $2\rho A$ we get

$$\frac{T}{2\rho A} = (V_C + v_i)v_i = V_C \cdot v_i + v_i^2 \tag{29}$$

where the left part of the above equation represents the square of induced velocity in hover, v_h^2,

$$v_h^2 = V_C \cdot v_i + v_i^2 \text{ or } \left(\frac{v_i}{v_h}\right)^2 + \frac{V_C}{v_h} \cdot \left(\frac{v_i}{v_h}\right) - 1 = 0 \tag{30}$$

The valid solution of the above equation is the positive ratio v_i / v_h

$$\frac{v_i}{v_h} = -\frac{1}{2}\frac{V_C}{v_h} + \sqrt{\frac{1}{4}\left(\frac{V_C}{v_h}\right)^2 + 1} \tag{31}$$

The product of the thrust and the total velocity through the rotor disc represents the power consumed, that is

$$P = T(V_c + v_i) = T \cdot V_C + T \cdot v_i = P_{c\lim b} + P_i \tag{32}$$

Vertical descent

In figure 19 is presented the vertical descent, where the air enters the stream tube from below the rotor with velocity V_D and passes through the rotor disc with the velocity $V_D - v_i$, the wake being formed with velocity $V_D - w$. The conservation of momentum gives the thrust force taking into account that the mass flow rate in vertical descent is $\dot{m} = \rho A(V_D + v_i)$ where V_D is negative, a

$$\begin{aligned} T &= \iint_{\substack{control\\surface}} (\rho\vec{V})\vec{V} \cdot d\vec{S} = \iint_{surface\ 1} (\rho\vec{V})\vec{V} \cdot d\vec{S} + \iint_{\substack{lateral\\surface}} (\rho\vec{V})\vec{V} \cdot d\vec{S} + \iint_{surface\ 2} (\rho\vec{V})\vec{V} \cdot d\vec{S} = \\ &= -\iint_{surface\ 1} \rho V_D \cdot V_D \cdot dS + 0 + \iint_{surface\ 2} \rho(V_D - w)(V_D - w) \cdot dS = -\dot{m}V_D + \dot{m}(V_D - w) = -\dot{m} \cdot w \end{aligned} \tag{33}$$

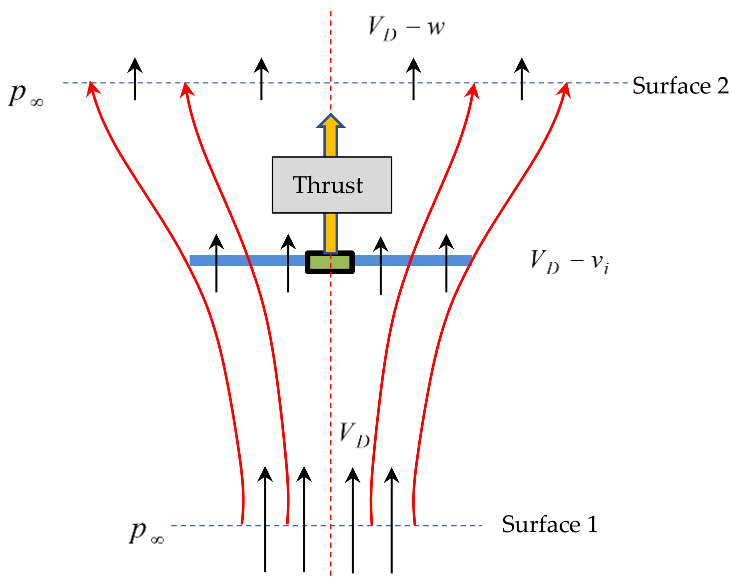

Fig. 19 The stream tube in descent.

Aplying the conservation energy principle it follows that

$$\begin{aligned} T \cdot (V_D - v_i) &= \iint_{\substack{control\\surface}} \left(\rho \frac{1}{2} V^2\right)\vec{V} \cdot d\vec{S} = \iint_{suface\ 1} \left(\rho \frac{1}{2} V^2\right)\vec{V} \cdot d\vec{S} + \iint_{\substack{lateral\\surface}} \left(\rho \frac{1}{2} V^2\right)\vec{V} \cdot d\vec{S} + \\ &\iint_{surface\ 2} \left(\rho \frac{1}{2} V^2\right)\vec{V} \cdot d\vec{S} = -\iint_{suface\ 1} \frac{1}{2} \rho V_D^2 \cdot V_D \cdot dS + 0 + \iint_{surface\ 2} \frac{1}{2} \rho (V_D - w)^2 (V_D - w) \cdot d\vec{S} = \\ &= -\frac{1}{2} V_D^2 \cdot \dot{m} + \frac{1}{2}(V_D - w)^2 \cdot \dot{m} = -\frac{1}{2}\dot{m}\left[V_D^2 - (V_D - w)^2\right] = -\frac{1}{2}\dot{m}\left(2V_D w - w^2\right) = \\ &-\frac{1}{2}\dot{m}w(2V_D - w) \end{aligned} \tag{34}$$

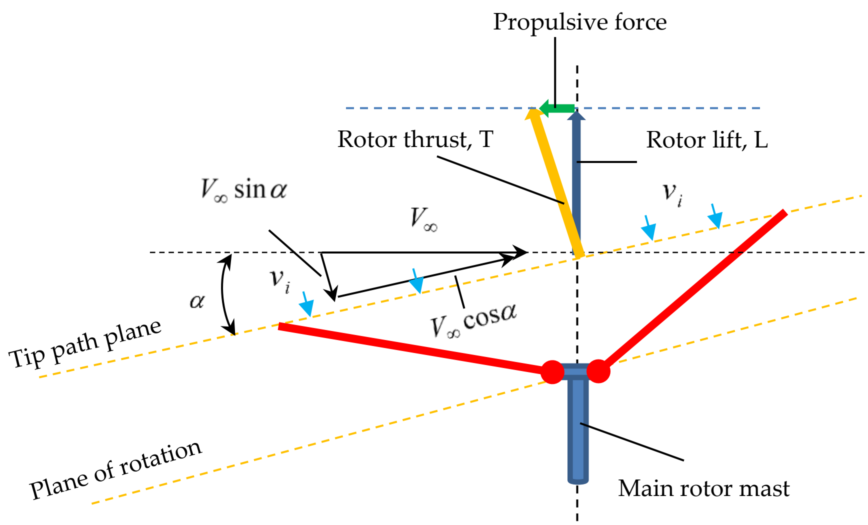

Fig. 20 Rotor in forward flight.

For the forward flight it is necessary to define two coefficients: *the advance ratio*, μ, and *the inflow ratio*, λ.

2.2.3 Helicopter systems

The lift is constantly changing through each revolution of the rotor, due to the difference in relative airspeed between the advancing and retreating blades, in forward flight, the asymmetry of the dynamic pressure over the disc, produces aerodynamic forces that are function of the blade azimuth position and in hovering flight, the blades flap up and lag back with respect to the hub and reach equilibrium position under the action of aerodynamic and centrifugal forces. In figure 21 is represented the flapping, lead-lag and feathering motion of a rotor blade

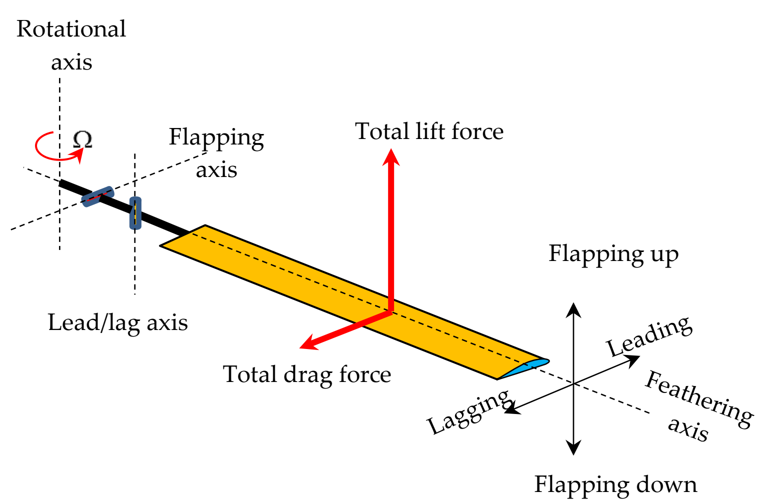

Fig. 21

2.2.4 Coaxial rotors systems – characteristics and performances

Based on the fluid dynamics and aerodynamics principles I built the mathematical model for the coaxial helicopter rotor and I pointed out that the induced power ratio relative to the power required to operate the two isolated rotors and the coaxial rotors are in favor of the later constructive solution. Despite of the constructive technological solutions, an advantage of this type of rotor is that it eliminates the need for a tail rotor by using counter rotating main rotors, where the net size of the rotors is reduced because each rotor provides vertical thrust and all power can provide vertical lift and helicopter control. The yaw control is accomplished by increasing the collective pitch of one rotor and decreasing the collective pitch of the other.

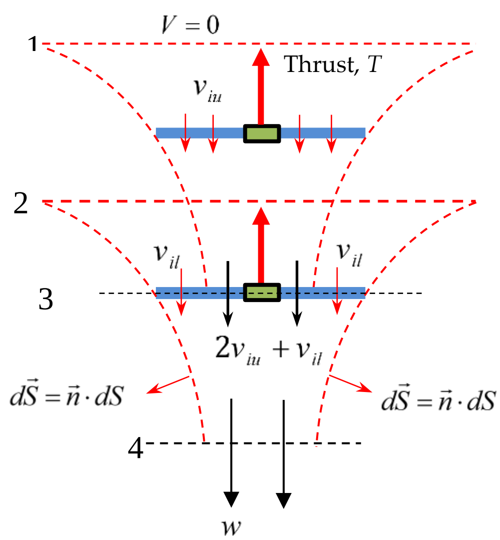

Fig. 22 Control volume for the coaxial rotors

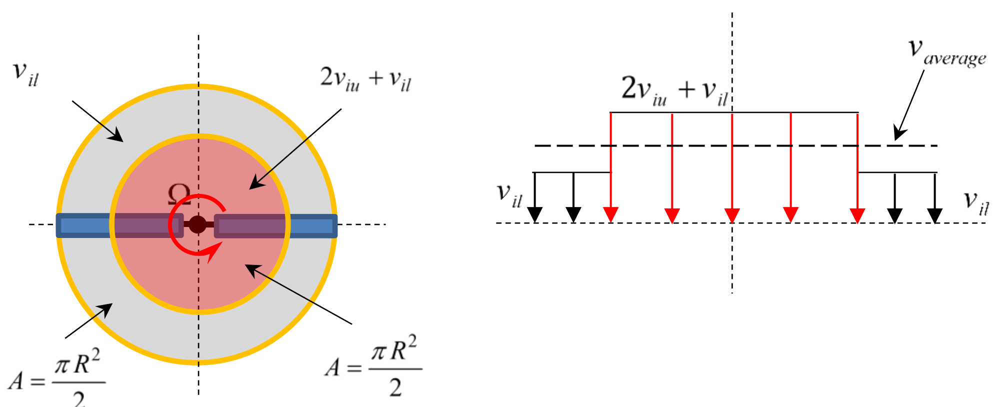

a) b)

Fig. 23

In figure 23b is presented the flow model applied to the lower rotor and according to the momentum equation, the rotor thrust is

$$\vec{T}_l = \iint_{S_4} \rho\left(\vec{V}\cdot d\vec{S}\right)\vec{V} - \iint_{S_2} \rho\left(\vec{V}\cdot d\vec{S}\right)\vec{V} = \dot{m}_l\,\vec{w} - \dot{m}_u\left(2\vec{v}_{iu}\right) \tag{35}$$

By replacing the mathematical expressions of the mass flow rate, it in the above equation, one can get

$$T_l = \rho A\left(v_{iu} + v_{il}\right)w - \rho A v_{iu}\left(2v_{iu}\right) = \rho A\left(v_{iu} + v_{il}\right)w - T_u \tag{36}$$

that leads to the equation

$$T_l + T_l = \rho A\left(v_{iu} + v_{il}\right)w \tag{37}$$

The unit vector $\vec{n}$ is oriented outward of the current tube, that is in front of the second integral in equation (35) appears the sign minus and on the lateral surface of the control volume, the double integral is zero because the vectors $d\vec{S} = \vec{n}\cdot dS$ and $\vec{V}$ are perpendicular, also, the work on unit time, namely the power consumed by the rotor for gaining in kinetic energy is obtained from the equation,

$$\begin{aligned} P_l = &\iint_{\substack{controll\\ surface}} \left(\rho\frac{1}{2}V^2\right)\vec{V}\cdot d\vec{S} = \iint_{suface\ 4} \left(\rho\frac{1}{2}V^2\right)\vec{V}\cdot d\vec{S} + \iint_{\substack{lateral\\ surface}} \left(\rho\frac{1}{2}V^2\right)\vec{V}\cdot d\vec{S} + \\ &+ \iint_{surface\ 2} \left(\rho\frac{1}{2}V^2\right)\vec{V}\cdot d\vec{S} = \frac{1}{2}\dot{m}_l V^2\Big|_{surface\ 4} + 0 - \frac{1}{2}\dot{m}_l V^2\Big|_{surface\ 2} \end{aligned} \tag{38}$$

In section 2 the velocity is zero in the outside of the upper rotor current tube and $2v_{iu}$ on the inner part of this current tube (fig. 22), that leads to the following expression for the power P_l,

$$P_l = \frac{1}{2}\underbrace{\left[\rho A\left(v_{iu} + v_{il}\right)\right]}_{\dot{m}_l} w^2 - \frac{1}{2}\underbrace{\left(\rho A v_{iu}\right)}_{\dot{m}_u}\left(2v_{iu}\right)^2 = \frac{1}{2}\rho A\left(v_{iu} + v_{il}\right)w^2 - 2\rho A v_{iu}^3 \tag{39}$$

Taking into account that on the inner part of the lower disc the air velocity is $2v_{iu} + v_{il}$ and on the other half part the air velocity is v_{il}, the average velocity is obtained as a medium velocity, as it follows

$$v_{average} = \frac{\frac{A}{2}v_{il} + \frac{A}{2}\left(2v_{iu} + v_{il}\right)}{\frac{A}{2} + \frac{A}{2}} = v_{iu} + v_{il} \tag{40}$$

hence, the lower rotor power consumed, has the expression

$$P_l = T_l\left(v_{iu} + v_{il}\right) \tag{41}$$

Applied this mathematical expression to the lower rotor, one can get,

$$T_l\left(v_{iu} + v_{il}\right) = \frac{1}{2}\rho A\left(v_{iu} + v_{il}\right)w^2 - 2\rho A v_{iu}^3 \tag{42}$$

or, taking into account the equation for the thrust force, it follows that

$$T_l\left(v_{iu} + v_{il}\right) = \frac{1}{2}\left(T_l + T_u\right)w - T_u v_{iu} \tag{43}$$

2.3 MATHEMATICAL MODELS APPLIED TO THE AIRCRAFT GAS TURBINE ENGINES

2.3.1 Human pilot's dynamic response characteristics

One important mathematical model which was studied and applied in different works and studies is one which analyses the system "pilot-aircraft-engine" as an integrated ensemble, being pointed out the handling qualities and the main pilot's abilities for aircraft command. In the habilitation thesis are presented two compensatory models, starting from the transfer functions of the aircraft dynamics. The airplane dynamic handling quality requirements were predicted on the basis of the methodology that shows the pilot models, tailoring the pilot's tasks, limitations, capabilities and human interactions across a range of possible operating conditions. No single modelling architecture had the objective to approaches the full range of interacting factors driving human actions in a complex and dynamic environment, like the flight of aircrafts.

PILOT MODEL

Due to the complex nature of the airspace field it is possible to model the aircraft-pilot system in many ways taking into account the real time control, despite the continual development of sophisticated data processing and communication technology applied to both military and commercial aviation. In figure 48 is presented one of the most successful approaches to the measurement problems of signal circulating in the control loop which utilizes power spectral density, where the human pilot is replaced by a mathematical model consisting of a linear describing function $Y(s)$ and a remnant, $n(t)$, which is considered because a linear model is never able to describe the pilot completely and it represents the signal that must be added in order to have all the time signals circulating in the system. The $Y(s)$ describes the pilot in any particular task and the remnant is chosen so as to minimize that part of the input signal to the aircraft which arises from $n(t)$. In this situation the linear pilot model that is obtained, is that which accounts for as much pilot input to the aircraft as possible. A measure of its adequacy can be considered the fraction of the pilot input to the aircraft accounted for by $Y(s)$.

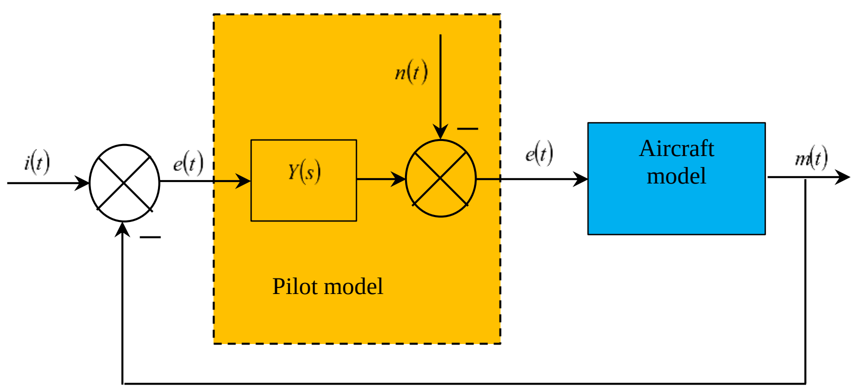

Fig. 24. Linear model of the pilot-aircraft system.

The control of the aircraft response, $m(t)$ is made by the pilot by viewing the instantaneous error $e(t)$, obviously, the pilots' control technique being influenced by the type of the input $i(t)$, the type of the display and the dynamics of the aircraft.

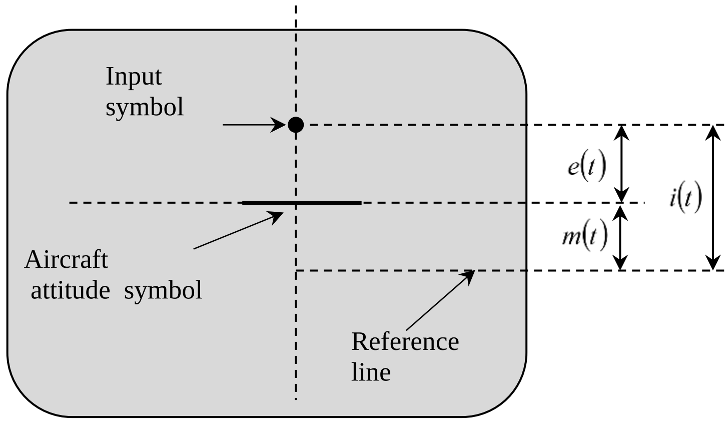

Fig. 25. Displayed variables.

Even if $e(t)$ is available in both cases, the information to the pilot are received after that the pursuit display separates the error into its components and conveys this information to the pilot. In the compensatory task, the single degree of freedom tracking task with a pursuit display is identical, except that the displayed variables are different.

2.3.2 Human pilot mathematical model

In order to analyze the aircraft's flying qualities, it is compulsory to have a mathematical representation of the pilot, which can be represented in a transfer function form that relates the pilot control output in response to perceived error in the aircraft's response to the desired command, having the following representation,

$$Y_p = K_p \frac{T_L \cdot s + 1}{T_I \cdot s + 1} \cdot \frac{e^{-\tau \cdot s}}{T_P \cdot s + 1} \tag{44}$$

The amount of control the pilot command in proportion of the perceived error is given by the first element of the transfer function, namely the gain, K_p . Dynamic compensation is represented by the T_L - lead time constant and lag T_I - lag time constant, according the above expression (44). The parameter τ represents mental processing and visual observation and this includes the elements that cannot be adjusted. Also, in the equation (44), the human muscle structure which cannot respond instantaneously to command to move and exhibit a lag in response, is represented by the term T_p . The observed variation of the T_p with forcing function bandwidth ranges from $0.1\,s$ to $0.6\,s$ and the time delay expressed by the $e^{-\tau \cdot s}$ term is due to the nerve conduction, sensor excitation, computational lags and other data processing activities in the central nervous system. The parameter τ is approximated as an invariant with controlled element dynamic and forcing function for either single or dual random-appearing inputs tasks. The order values for time delay are $\tau = 0.2\ s$ and the time lag T_p is approximately $0.1\ s$.

2.3.3 Mathematical models applied to the turbojet engines

In order to study the main characteristics and optimal parameters of turbojet engines I built up the mathematical models, based on the general theory for nonlinear systems where the constrained optimization problems were formulated taking into account matrix formulas for Maple environment.

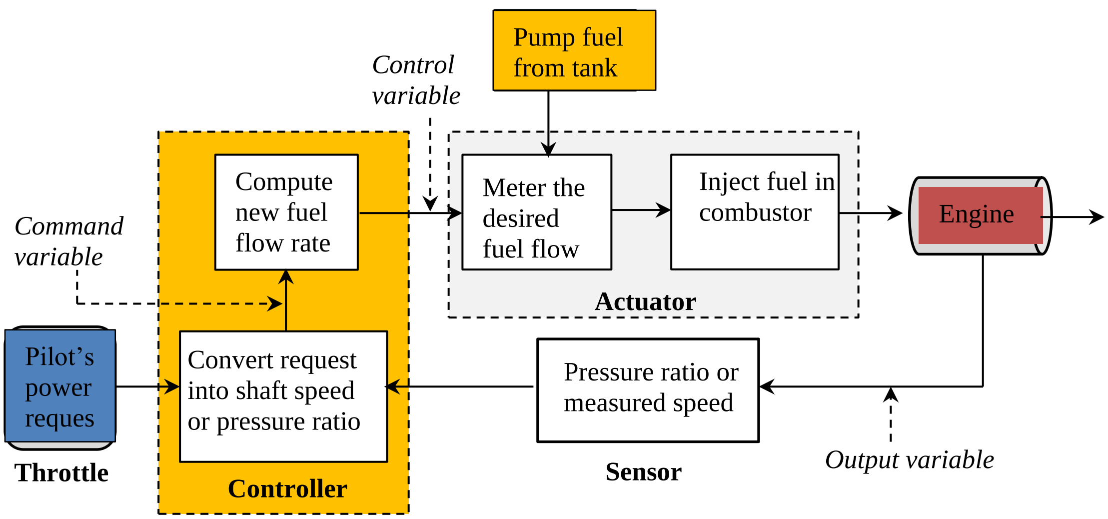

Fig. 26. Engine control system diagram

The complexity of the control system can be evaluated by the number of control variables or by the number of measured variables in the system, which corresponds directly to the number of actuators and the number of measured variables to the number of sensors.

In the following picture is presented the corrected fuel flow for the main burner,

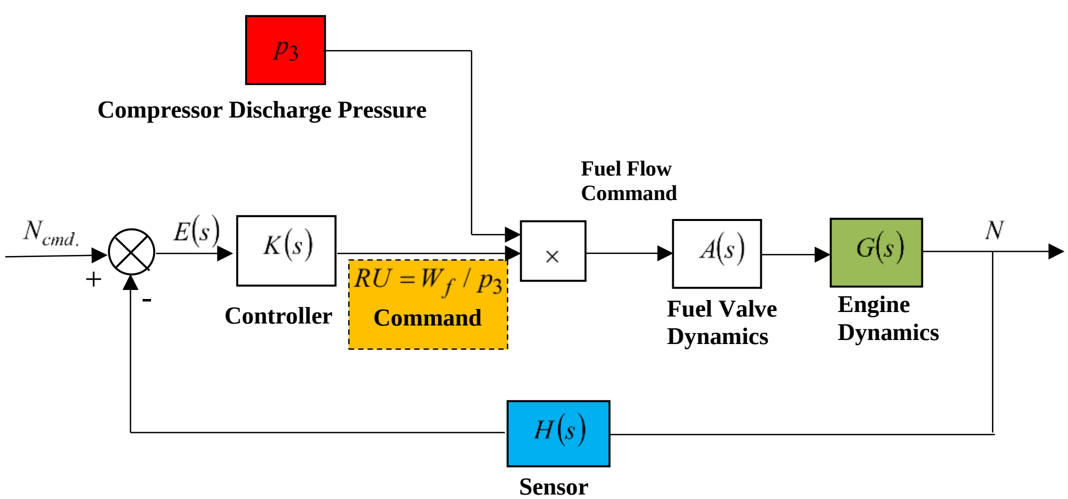

Fig. 27. Controller output to main burner fuel flow rate

2.3.4 Engine operability limits

For a compressor map coordinates, unique values for rotor speed and efficiency exist, the coordinates of a point of a point in the in the compressor map correspond to steady-state operation at some pressure ratio and mass flow rate.

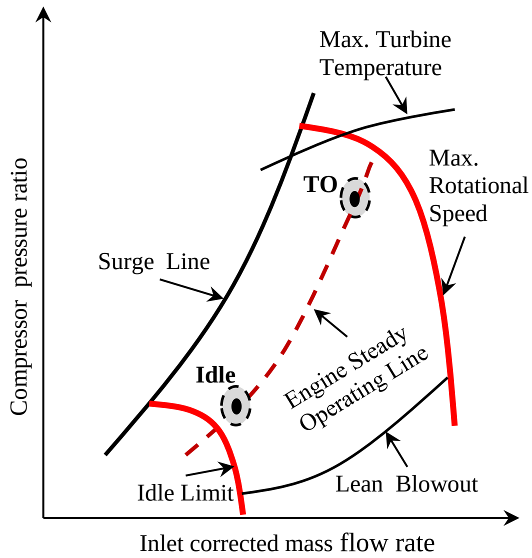

Fig. 28. Engine operating limits on compressor map

If pressure and heat release are in phase, perturbations are introduced to a steady flow condition so that, resonant oscillations are induced.

2.3.5 Reduced order mathematical model

The engine model can be express by a time variant model within a finite time interval near a nominal operating point. Based on this linear model, we can derive a reduced-order model that is more suited for control laws designs and we also can analyze the dynamics of the engine because the model can result in overly complex control laws that are sensitive to parameters variations and modeling uncertainties.

$$\begin{cases} \dot{\tilde{x}} = \Lambda \tilde{x} + \tilde{B} u \\ y = \tilde{C} \tilde{x} + \tilde{D} u \end{cases} \tag{45}$$

where $\tilde{x}$ is related to the original state variables by the canonical transformation matrix *T*, such that $x = T\tilde{x}$, being the vector that contains modal state variables and where $\Lambda = T^{-1}AT$ is an $n \times n$ diagonal matrix with the eigenvalues of *A* the roots of the characteristic equation of the transfer function from input u to output *y*. The above equation can be transformed into a set of *r* reduced states $\tilde{x}_1$ and $(n-r)$ remaining states $\tilde{x}_2$ as

$$\begin{cases} \begin{bmatrix} \dot{\tilde{x}}_1 \\ \ldots \\ \dot{\tilde{x}}_2 \end{bmatrix} = \begin{bmatrix} \Lambda_1 & | & 0 \\ \ldots & \ldots & \ldots \\ 0 & | & \Lambda_2 \end{bmatrix} \begin{bmatrix} \tilde{x}_1 \\ \ldots \\ \tilde{x}_2 \end{bmatrix} + \begin{bmatrix} \tilde{B}_1 \\ \ldots \\ \tilde{B}_2 \end{bmatrix} u \\ y = \begin{bmatrix} \tilde{C}_1 & | & \tilde{C}_2 \end{bmatrix} \begin{bmatrix} \tilde{x}_1 \\ \ldots \\ \tilde{x}_2 \end{bmatrix} + \tilde{D} u \end{cases} \tag{46}$$

where Λ_1 is an $r \times r$ diagonal matrix and Λ_2 is an $(n-r)\times(n-r)$ diagonal matrix.

2.3.6 Mathematical model for partially premixed combustion

The most important elements of jet engines are the step blade rows where the whole flow is the result of blades network which impart the force and more relevantly, the moment of the flow. The temperature distribution randomness causes the first stator stage to be designed for the maximum temperature of fluid coming out of the combustor (Fig. 29).

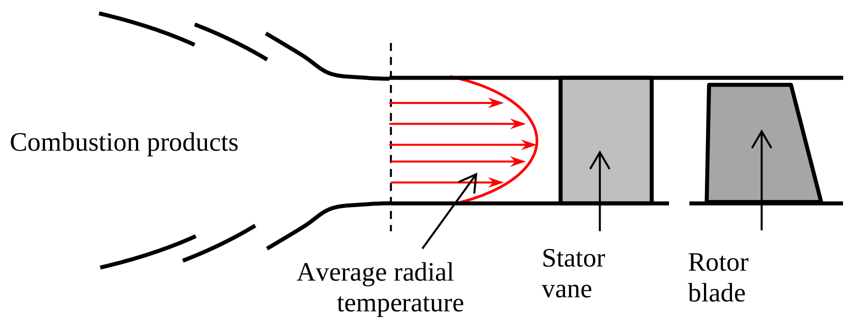

Fig. 29 Turbine blade radial temperature profile

The heat transfer coefficient distribution over a hole airfoil must be known in detail and at the stagnation point this coefficient can be correlated as that of the stagnation point of a cylinder in a cross flow that is affected by the freestream turbulence. The boundary layer trips to turbulent flow on the concave side of the blade airfoil and attains a heat transfer coefficient level corresponding to a low Reynolds number turbulent flow.

(a) (b)

Fig. 30. The jet engine model (a) and the combustor shape (b)

In the jet engines, three-dimensional flows are encountered with unfortunate regularity in the boundary layers and the freestream and in the pitch averaging approach, the azimuthal variations are expressed as a mean value plus a small perturbation and the equations of motion averaged in the azimuthal direction.

2.3.7. Numerical methodology for CFD calculation

The separated flow regions interacting with an inviscid outer flow region have a basic structure model that leads to considerable economy of computation relative to solving the full Navier-Stokes equations. A single scalar potential equation may be used if the external flow can be assumed irrotational, and the correction perturbation to this inviscid outer flow may be obtained from linearized theory, but the interacted boundary layer is not well posed as an initial value condition, while he conventional boundary layer approach leads to a parabolic system of equations. The interacting boundary layer has the following governing equations

$$\begin{cases} (\rho u)_x + (\rho u)_y = 0 \\ \rho u u_x + \rho v u_y = -p_x - (\mu_T u_y)_y \end{cases} \quad (47)$$

where x and y subscripts denote differentiation, u and v are the velocities, μ_T is the sum of the laminar and turbulent effective viscosity, p_x is the pressure gradient and ρ is the gas density.

The boundary conditions for these equations are

$$\begin{cases} y = 0, \ u = v = 0 \\ y = \delta, \ \ p = p_e(x) \end{cases} \quad (48)$$

where δ is the thickness of boundary layer.

The effects of the Coriolis and centrifugal forces on the mean flow are negligible because the rotating external blade boundary layer are very thin. In the following pictures are presented some important CFD results regarding the flame tube geometrical shapes.

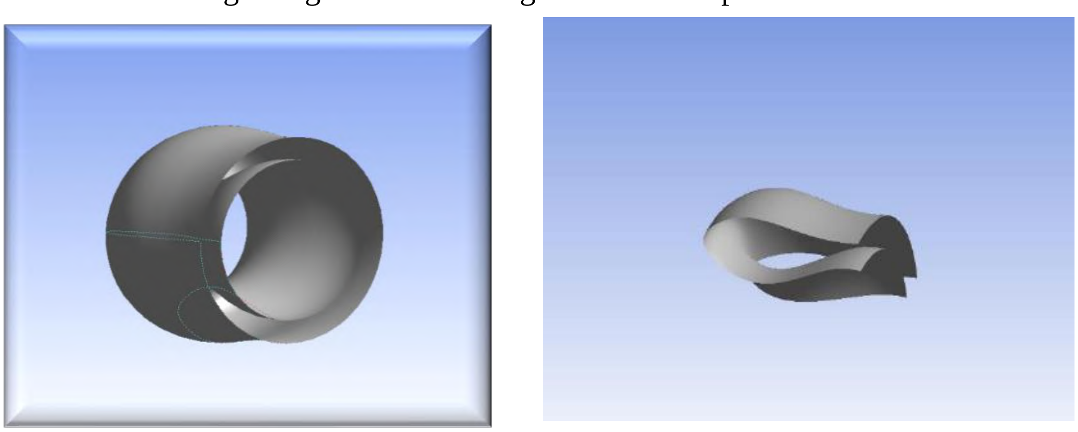

(a) (b)

FIG. 31. The 3D view (a) and lateral view (b) of the flame tube

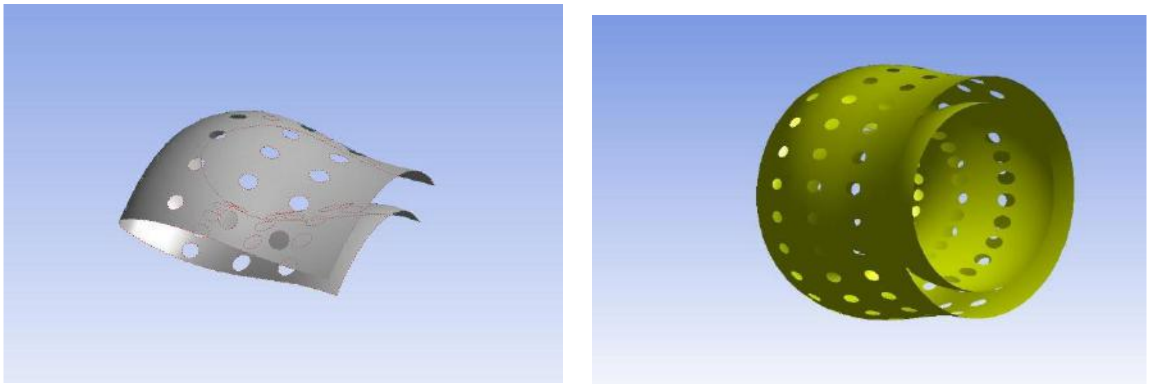

(a) (b)

FIG. 32. The external hole distributions, quarter view (a) and 3D view (b)

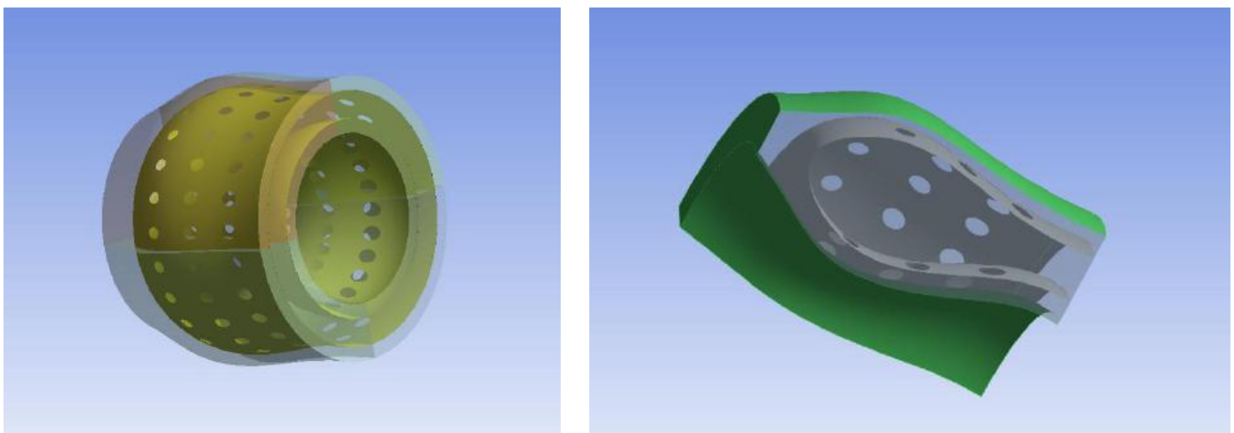

(a) (b)

FIG. 33. Geometrical shape (a) and internal view (b)

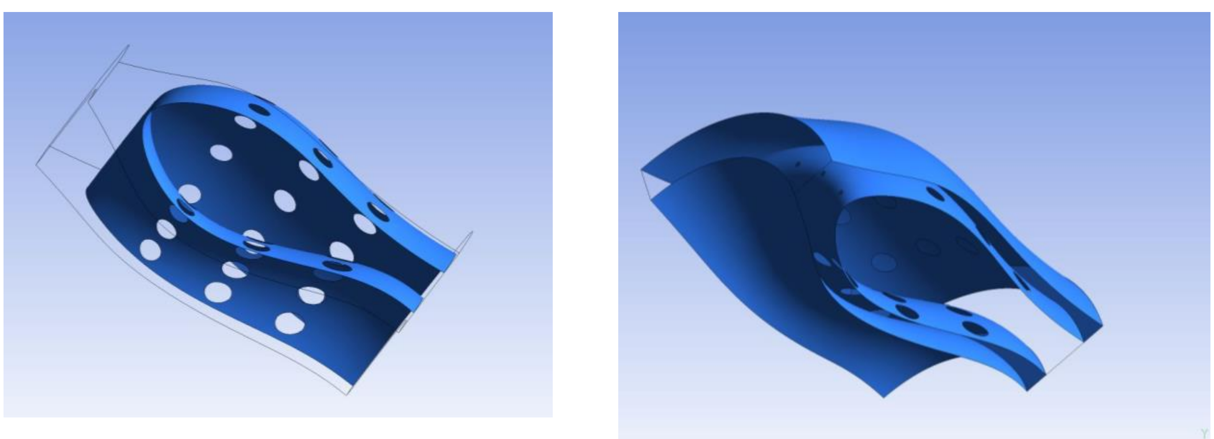

(a) (b)

FIG. 34. The contour of the inlet section (a) and the injectors holes (b)

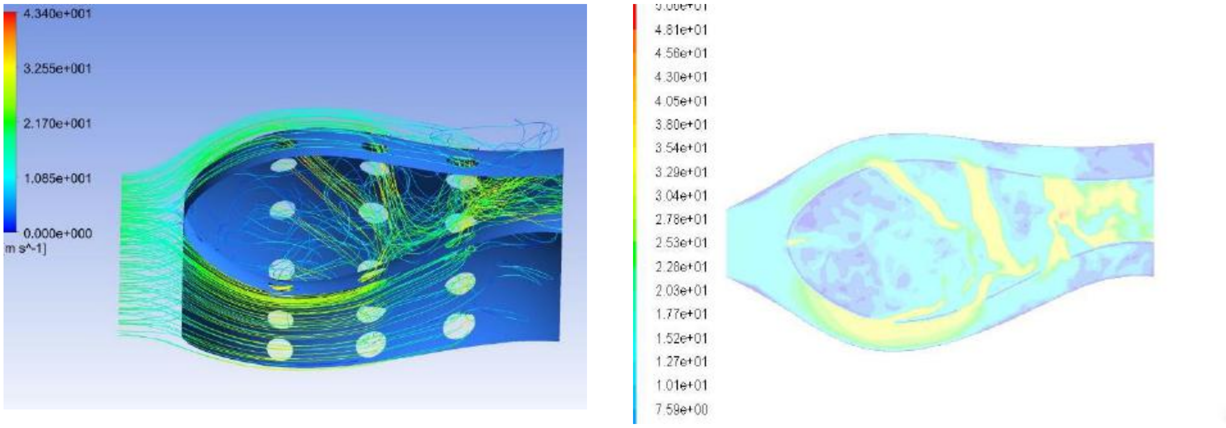

(a) (b)

FIG. 35. The inner stream lines (a) and velocity distribution (b)

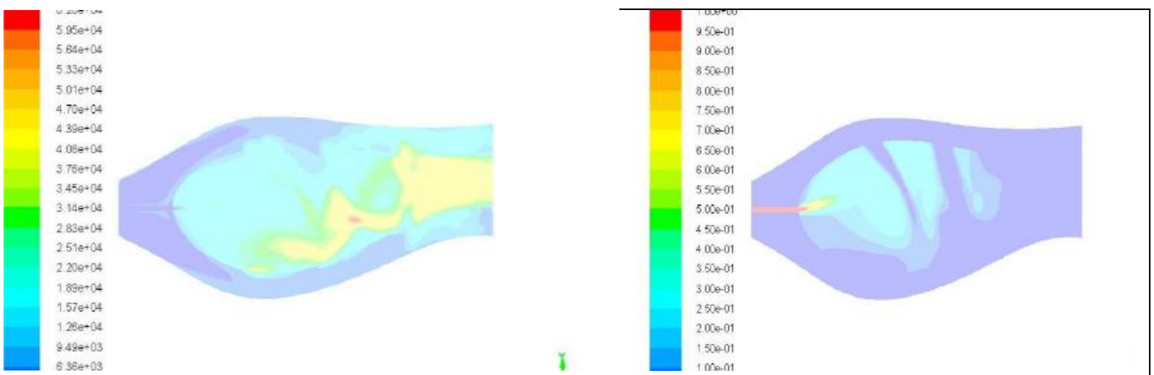

(a) (b)

FIG. 36. Turbulent intensity (a) and Mass fraction of jet A fuel (b)

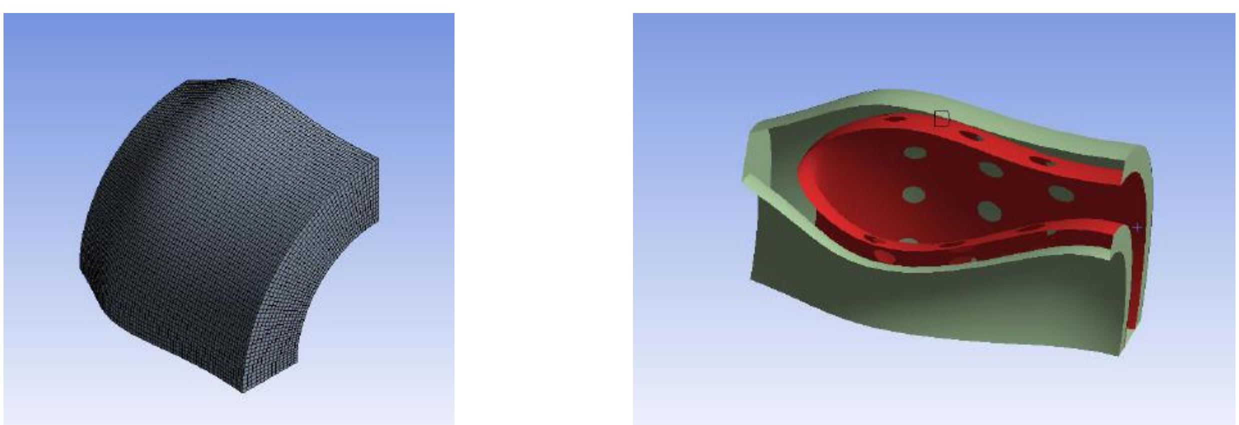

(a) (b)

Fig. 37. The mesh domain (a) and flame tube wall position (b)

The combustion model used to describe the burning process in an annular flame tube has the advantage of cleanly separating aerodynamic and chemical features of the process and the chemical concentrations and temperature used in the combustion chamber are taken from a mathematical model of the mixing zone that is based on time-averaged measurements.

2.3.8 An extended combustion model

One important research direction consisted in modelling and simulation of the combustion in a turbojet engine in order to find the optimal shape of combustion chambers and the optimal characteristics of the burning process and also to find a new configuration of the aircraft engine combustion chambers.

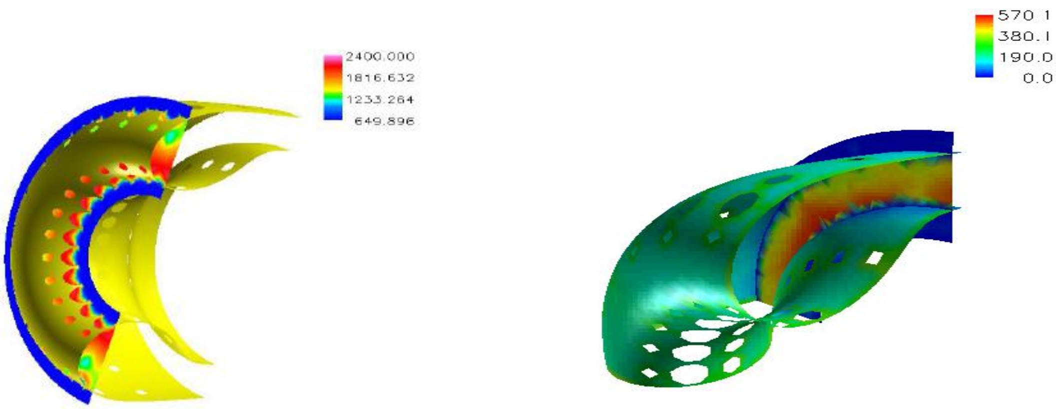

Temperature in the flame tube

Velocity magnitude in the flame tube

Fig. 38

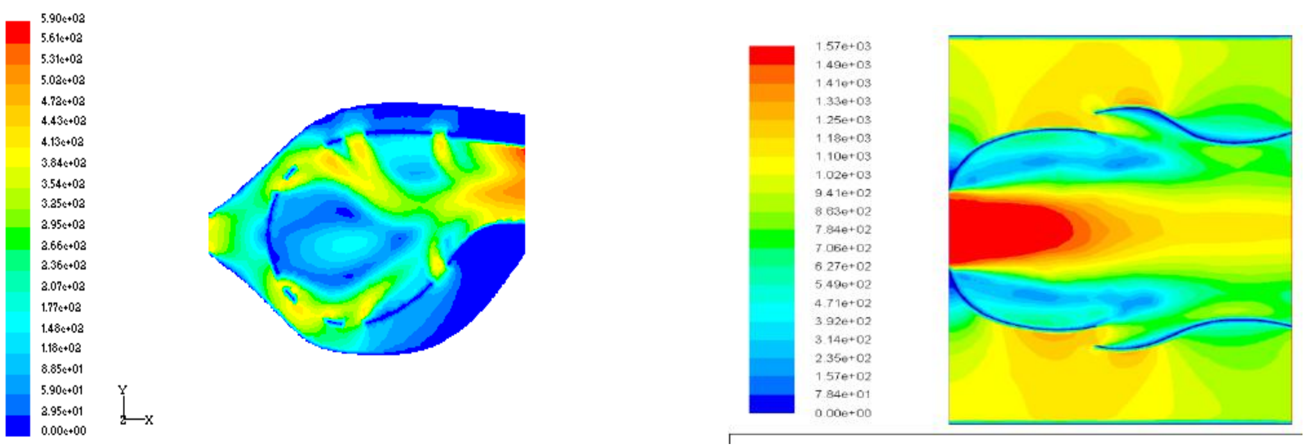

Velocity contour în the flame tube

Contours of velocity magnitude in the second combustion chamber

Fig. 39

For laminar one dimensional premixed flames the simplified conservation equations are

$$
\begin{aligned}
&\frac{\partial \rho}{\partial t}+\frac{\partial(\rho u)}{\partial x}=0\\
&\frac{\partial \rho Y_k}{\partial t}+\frac{\partial}{\partial x}\left[\rho(u+V_k)Y_k\right]=\dot{\omega}_k\\
&\rho C_p\left(\frac{\partial T}{\partial t}+u\frac{\partial T}{\partial x}\right)=-\sum_{k=1}^{N}h_k\dot{\omega}_k+\frac{\partial}{\partial x}\left(\lambda\frac{\partial T}{\partial x}\right)-\rho\frac{\partial T}{\partial x}\left(\sum_{k=1}^{N}C_{p,k}Y_kV_k\right)
\end{aligned}
\qquad (49)
$$

where ρ - mixture density, $\dot{\omega}_k$ is the reaction rate , Y_k is the mass fractions of species k in the reaction mixture, λ - heat diffusion coefficient, u axial velocity, V_k is the diffusion velocity, , C_p and $C_{p,k}$ are the heat capacities at constant pressure of the mixture and of the species k respectively, h_k the enthalpy, T – temperature. The boundary conditions are $u|_{x=0}=u_1$, $T|_{x=0}=T_1$ and also, the flame must be ignited and the temperature must reach the adiabatic flame temperature at the outlet of the flow domain.

For one-dimensional reactive flow the basic model configuration is presented in the fig. 40.

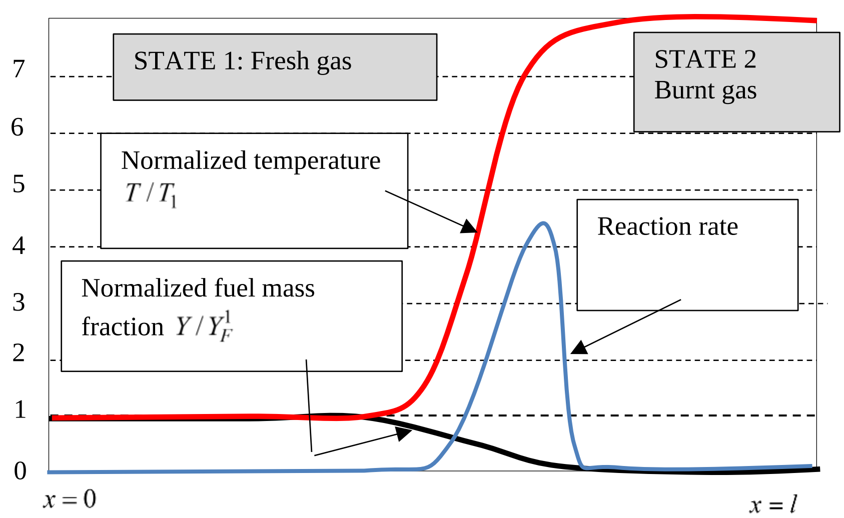

Fig. 40. Combustion computation model

The reduced reaction rate, expressed by $\dot{\omega}_F/\left(\rho_1 Y_F^1 B_1\right)$ is a function of only one variable, θ, and it has a maximum value for $\theta = 1-1/(\alpha+\beta)$. In figure 90 are presented four lines corresponding to $\alpha = 0.75$ and different β_1 and β exponents.

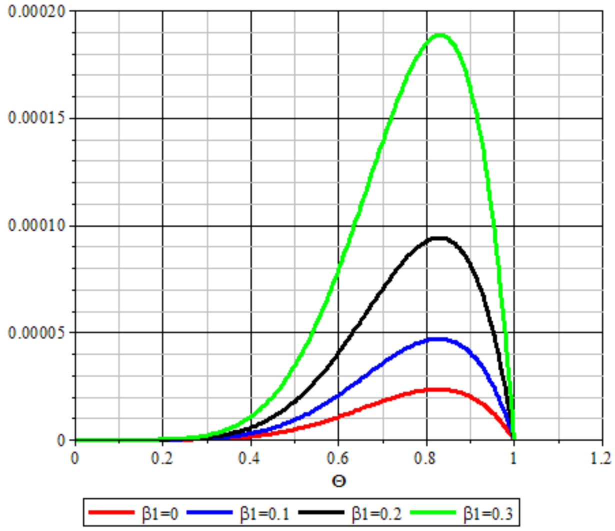

(a)

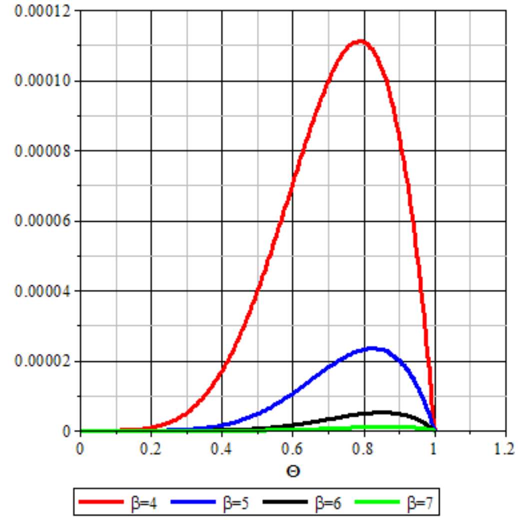

(b)

Fig. 41. The reduced reaction rate for $\beta = 5$ (a) and $\beta_1 = 0$ (b)

The flame velocity remains at $x_f = 0$ for stoichiometric conditions, and it is moving toward the fuel for $\varphi < 1$ and toward the oxidizer for $\varphi > 1$. Taking into account the conservation equation for fuel,

$$\frac{\partial \rho Y_F}{\partial t} + \frac{\partial}{\partial x_i}(\rho u_i Y_F) = \frac{\partial}{\partial x_i}\left(\rho D \frac{\partial Y_F}{\partial x_i}\right) + \dot{\omega}_F \qquad (50)$$

in the case of constant density and zero velocity flow, the fuel reaction rate per unit flame area, $\dot{\Omega}_F$, can be obtained by integrating $\dot{\omega}_f$ between two points located on both sides of the flame front, delimited by x_f on the right and the left sides:

$$\dot{\Omega}_f = -\int_{x_f^-}^{x_f^+} \frac{\partial}{\partial x_i}\left(\rho D \frac{\partial Y_F}{\partial x_i}\right) dx = -\frac{\rho}{2} \frac{Y_F}{1 - z_{st}} \sqrt{\frac{D}{\pi t}} e^{-\eta_t^2} \qquad (51)$$

The asymmetric distribution of the holes surface assures a higher turbulence in the secondary area, therefore, the residence time of the air–fuel mixture in the combustion chamber is higher, which allows the complete burning of this mixture.

3. Conclusions and career development plan

The professional experience gained in the activity performed in aviation bases, research and higher education institutes is an important argument for the development of complex technical investigations. An overview and knowledge of aviation systems and subsystems are two essential requirements for approaches to scientific topics in the field of aerospace. My collaboration with scientific researchers from the country and from abroad allowed me to approach multidisciplinary subjects, boundary topics, of perspective, with direct practical applications. My career development plan of is based on my scientific activity and is structured into short, medium and long term.

There are three main directions in which I will further do my research:

- Development of mathematical models for extending the study area around geometric bodies similar to those of airplanes and helicopters, aircraft control surfaces, main rotor and tail rotor in helicopters;
- Identification of new constructive solutions for aeroreactive propulsion systems;
- The study of combustion chambers of turbojet engines and the application of the detonation phenomenon in supersonic combustion chambers.

Moreover, I will extend my research activities in the following fields:

- Vertical take-off and landing aircraft;
- Aerospace design and simulation.

My future research activity will represent an extension of the topics already addressed, a continuation of the topics that have produced results. For example, the results obtained in the project "Microlauncher based on the detonation engine" may be extended by applying the detonation phenomenon to the study of a propulsion system able to offer a much higher efficiency compared to the current propulsion systems used in aviation. Supersonic combustion will be able to offer new solutions for stator jet engines and it can also be applied to turbojet engines with supersonic turbine.

Regarding the courses that I taught as a tenure-holder at the Military Technical Academy and at “Henri Coandă” Air Force Academy, respectively *Airplane and helicopter aerodynamics, Flight mechanics, Aviation engine theory, Aircraft construction and operation, Automation of aviation engines*, for the Bachelor’s degree programs and *Aerothermodynamics*, for the Master’s program, I hold as a fundamental objective to permanently improve the content and quality of the educational act. Thus, first of all, I consider the continuation and intensification of the personal effort to adapt the courses that I proposed to the current requirements of the beneficiaries and in general, to the demands of the labor market in the field. In this context, from the perspective of the didactic material development for Bachelor’s and Master’s students, etc., I forward the following objectives of interest:

✓ For the course of *Aerodynamics and Mechanics of Aircraft Flight* I want to continue the series of specialized works published, with two new titles, namely: *Fundamentals of Aerodynamics* and, respectively, a course in English dedicated to pilot Bachelor’s students, *Dynamics of Flight*. Basically, after the presentation in the volumes already published of the fundamental theoretical and applicative elements specific to the fundamentals of aerodynamics and piloting, the two new works will achieve, through their content, a particularization of the general principles of the dynamics of the flight and of the minimum mathematical support for performing calculations, numerical simulations and the use of software programs dedicated to aerospace applications. For the course of *Aircraft Construction and Operation*, I want to continue the series of specialized books in the field, by publishing a volume that represents, through its content, an encompassing of all the installations and equipment that make up the aircraft, focusing on the specific installations of military aircraft. I must point out that this objective is not a mere desiderate, at present it already has several chapters in an advanced stage of work.

From the perspective of the applicative part of this course, I want to continue improving the set of functions available within the currently used laboratory platforms. Also, this update will be achieved either through personal effort in some scientific research projects, or by involving Bachelor's and Master's and Doctoral students in new projects, dissertation and doctoral topics.

✓ In direct connection with the field of flight simulators, another direction of interest in my didactic and scientific activity will be the development of mathematical models specific to the dynamics of flight, able to perform simulations and interpretations of the special cases of flight, as well as a simple analysis of the flight parameters. Thus, having as support the consistent experience accumulated in this regard, I intend to, in collaboration with other colleagues of the department, elaborate a didactic manual and publish some articles on the automatic control of aircraft and flight simulators. Also, in an applicative manner, I intend to contribute to the increase of the package of functions existing within the laboratory platforms currently used, within these courses and following the same scientific directions of interest.

Another direction of interest from the perspective of my research activity is and will be represented by the field of *advanced computer-based design technologies, high-speed flow modeling and increasing the thrust of air-jet propulsion systems*. In this regard, I aim to initiate and finalize the specific debates within the specialized teaching commission regarding the introduction of specialized courses in the curricula of the study programs run within the department. My experience in this respect is a significant one and it supports my involvement in the development of specialized scientific works in collaboration with other colleagues, but also in the submission / development of scientific research projects in collaboration with prestigious companies in the aerospace field.

The academic scientific research is one of the most important activities at national and international level. It is an effective development tool and a necessity for the continuation of the didactic activity. From the perspective of the scientific research activity, the main future objectives that I have in mind are as follows:

✓ to continue the specific activity of *accessing funds* by carrying out *new scientific research projects* as a project manager / project member, both at national and European level. In this context, I will try to maximize the scientific connections I have accumulated so far, so that the Doctoral School of which I will be a part, can participate as a partner or coordinator, in as many scientific research projects as possible. Also, I will try to highlight as much as possible, the areas of unique scientific or strong expertise of the department or faculty.

- ✓ in the same line, I will contribute to the development of new directions of interest from the perspective of scientific research, within the department or faculty. Thus, personally, from the perspective of my accumulated experience, I will get involved in structuring a strong scientific research team in the field of *advanced modeling / simulation technologies*.
- ✓ publication of significant scientific results obtained in the *directions of interest* mainly, in specialized journals with relevant impact factor.
- ✓ from the perspective of the advanced numerical calculation technologies, I will focus in the future on the development and optimization of advanced mathematical models for describing the movement of the plane, for modeling its geometry in order to simulate flows at the highest precision.
- ✓ in the near future, I intend to strengthen the already existing scientific collaborations and to access new opportunities in this direction. Thus, both in the context of the development of new projects in the line of scientific research, and in the idea of improving the qualitative level of the educational act, I will consider the continuation or extension of personal scientific collaborations with other professors from the country, from abroad or with prestigious companies in the aerospace field.

In the end of this perspective plan regarding my didactic activity and scientific research, I would like to present, synthetically, the objectives considered by me as a top priority in this direction, namely:

- ✓ continuous improvement of the scientific content of the courses, at the same time with all efforts being made to modernize their material base;
- ✓ continuation of the scientific research activity by accessing mainly specialized magazines with a relevant scientific impact (preferably, ISI indexed), but also some scientific manifestations indexed ISI proceedings, etc.;
- ✓ raising funds within the doctoral school by developing new opportunities in the line of scientific research projects, both nationally and internationally.

Another aspect of interest for me will consist of assuring a natural continuity of my scientific research activity, including from the perspective of the publishing activity and of engaging in new scientific research projects. Also, I will continue to disseminate the results of my scientific research activity, mainly, to *specialized journals of high scientific impact*, because, as I mentioned before, the dissemination of the obtained results is in fact the main means of evaluating and recognizing the scientific prestige of a Doctoral supervisor, but also one of the main criteria for assessing the visibility of an educational institution.

4. References

1. J. D. Mattingly, "Elements of Propulsion. Gas Turbines and Rockets", AIAA, Reston Virginia, USA, 2006.
2. J. D. Mattingly, W. H. Heiser, D. T. Pratt, "Aircraft Engine Design",second edition, AIAA, Reston Virginia, USA, 2002.
3. S. Farokhi, "Aircraft Propulsion", John Wiley & Sons Inc., USA, 2009
4. L. C. Jaw, J. D. Mattingly, "Aircraft Engine Controls – Design, System Analysis and Health Monitoring", AIAA, Reston Virginia, USA, 2009.
5. R. F. Huang, H. F. Yang, C. M. Hsu, "Flame Behavior and Thermal Structure of Combusting Nonpulsating and Pulsating Plane Jets", Journal of Propulsion and Power, Volume 29, number 1, 2013, pag. 114-124
6. Yeshayahou Levy, Vladimir Erenburg, Valery Sherbaum, "Increasing Operational Stability in Low NOx GT Combustor Using Fuel Rich Concentric Pilot Combustor", International Journal of Turbo and Jet Engines, Vol. 29 (2012), pp. 9-19.
7. Y. Levy, V. Sherbaum, V. Erenburg, "Effect of the Recirculating Gases on the Mild Combustion Regime", International Journal of Turbo and Jet Engines, Vol. 26 (2009), pp. 9-18.
8. S. Nigam, D. Ahmed, A. Kushari, "Macroscopic Flow Behavior in a Low Aspect Ratio Dump Combustor with Tapered Exit", International Journal of Turbo and Jet Engines, Vol. 29 (2009), pp. 19-31.
9. Digvijay B. Kulshreshtha, S. A. Channiwala, "Kerosene Fuelled Tubular Type Combustion Chamber Gas Turbine Engine: Design Methodology and Numerical Investigations", International Journal of Turbo and Jet Engines, Vol. 27 (2010), pp. 63-78.
10. P. K. Ezhilkumar, D. P. Mishra, "Numerical Modeling of an Axisimmetric Trapped Vortex Combustor", International Journal of Turbo and Jet Engines, Vol. 28 (2011), pp. 41-52.
11. FLUENT Documentation.
12. C. J. Jaw, J. D. Mattingly, "Aircraft Engine Controls. Design. System Analysis and Health Monitoring", AIAA, Reston, Virginia, USA, 2009.
13. C. Rotaru, M. Mihăilă-Andres, P. G. Matei, "An Extended Combustion Model for the Aircraft Turbojet Engine", International Journal of Turbo&Jet Engines, ISSN 0334-0082, Vol. 31, Issue 3, Pages 229-237, doi: 10.1515/tjj-2013-0048, 2014.
14. T. V. Chelaru, A. Chelaru, "Reaction Control System using Hybrid Micro-Thrusters for Guides Sounding Rocket", Proceedings of the 6th International Conference on Recent Advances in Space Technologies – RAST 2013, pp. 837-842, ISBN:978-1- 4673-6394-5, Istambul, Turkey, 12-14 June, 2013.
15. C. Rotaru, I. Sprintu, "State variable modeling of the integrated engine and aircraft dynamics", 10th International Conference on Mathematical Problems in Engineering, Aerospace and Sciences ICNPAA 2014, Volume 1637, pp. 889-898, 2014.
16. H. Richter, "Advanced Control of Turbofan Engines", Springer Science, USA, 2012.
17. C. E. Moldoveanu, A. Giovannini, H. C. Boisson, "Turbulence receptivity of longitudinal vortex dominated flow", Lecture Notes in Computational Science and Engineering, Vol. 69: BAIL 2008-Boundary and Interior Layer Proceedings of the International Conference on Boundary and Interior Layers-Computational and Asymptotic Methods, Limerick, Springer Verlag, Berlin, pag. 227-236, ISBN: 978-3-642-00604-3, July, 2008;
18. A. N. Tudosie, "Supersonic Air Inlet Control System Based On The Inner Channel Minimum Cross-Section Position Control", International Conference on Military Technologies ICMT 2009, Brno, Czech Republic, 2009;
19. C. Rotaru, I. Cîrciu, C. Aramă, C. G. Constantinescu, "Aspects Regarding Velocity Distribution in the Secondary Zone of a Gas Turbine Combustor", Review of the Air Force Academy, No. 3(30), DOI: 10.19062/1842-9238.2015.13.3.5, pp. 33-37, 2015;
20. A. N. Tudosie, "Aircraft Jet Engine Exhaust Nozzle Controller Based on Turbine Pressure Ratio Sensor with Micro-Jet System", Proceedings of the 11th International Conference on Applied and Theoretical Electricity (ICATE), Craiova, 2012